



SAPIENZA  
UNIVERSITÀ DI ROMA



ARISTOTLE  
UNIVERSITY OF  
THESSALONIKI

# Fire and Sand: An archaeometric analysis of the Roman architectonic glass found during the excavation of Lamia's Gardens

Facoltà di Scienze Matematiche, Fisiche e Naturali

Corso di laurea in ARCHMAT (ERASMUS MUNDUS MASTER IN  
ARCHaeological MATerials Science)

Martha Parasoglou

Matricola 1946373

Relatore Dr. Laura Medeghini (Supervisor - Sapienza University of Rome)

Correlatore Dr. Pedro Barrulas (Co-supervisor - University of Évora)

Dr. Michella Botticelli (Co-supervisor – Sapienza University of Rome)

Rome, November 2021



## Abstract

This thesis presents the results of an archaeometric research performed, through a multi-analytical approach, on a series of Roman architectonic glasses dated from the second half of the 1st to the 2nd century AD and excavated in Lamia's Gardens, located in Rome. Chemical analyses of glass samples of different colours were performed to define the glass-making technology and study the raw material provenance. Optical microscopy and SEM-EDS were used to identify homogeneity and glass morphological features like bubbles, inclusions and corrosion. Chemical analysis was performed by SEM-EDS and EMPA for major and minor elements, whereas trace elements were analysed by means of LA-ICP-MS. The results obtained show that all the samples analysed have the typical composition of natron-lime-silica glass. Furthermore, the comparison between the samples analysed and known compositions of Roman glass demonstrated that the raw glass was produced in two different locations, possibly in Egypt and on the Syro-Palestinian coast.

## Acknowledgments

This M.A. thesis would not have been accomplished without the continuous support of supervisors, friends and family.

I would like to thank my supervisors for giving me the opportunity to participate in such an engaging project. I am grateful for their constant availability and encouragement.

I would also like to thank Prof. Nick Schiavon and the ARCHMAT International Selection Committee for accepting me in this master program and all the professors that contributed to obtain the necessary knowledge and skills for archaeometric research.

I also deeply appreciate all my friends and family for their support, encouragement and understanding.

## Table of Contents

Abstract.....	2
Acknowledgments.....	3
List of Figures.....	6
List of Tables .....	7
1. Introduction.....	8
1.1. Background of Study .....	8
1.2. Object of Study .....	9
1.3. Research aim .....	9
1.4. Overview of the chapters .....	10
2. Glass.....	12
2.1. Definition .....	12
2.2. Raw Materials.....	12
2.2.1. Network former .....	12
2.2.2. Fluxes .....	13
2.2.3. Stabilizers .....	14
2.2.4. Fining agents.....	14
2.2.5. Colourants and decolourants.....	14
2.2.6. Opacifiers.....	15
2.3. Production of glass.....	16
2.4. History of glass production and glass making techniques .....	17
2.4.1. Early glass production .....	17
2.4.2. Glass production during the Hellenistic period.....	18
2.4.3. Roman glass production.....	19
2.5. Architectonic glass .....	23
3. Lamia’s Gardens .....	25
4. Materials and methods.....	32
4.1. Materials.....	32
4.2. Methods.....	37
4.2.1. Sample preparation.....	37
4.2.2. Analytical Methods.....	37
5. Results .....	41
5.1. Macroscopic and microscopic analysis .....	41
5.2. SEM-EDS.....	50
5.3. EMPA.....	56
5.4. LA-ICP-MS.....	59

6. Discussion.....	62
6.1. Glass-making Technology.....	62
6.1.1. Colourants and Decolourants .....	64
6.1.2. Opacifiers.....	70
6.1.3. Recycling of glass .....	71
6.2. Provenance.....	72
7. Conclusion .....	76
Bibliography .....	78

## List of Figures

Figure 3.1 The Gardens of Rome in green, the area of Lamia's Gardens in the red circle (Cima and Talamo, 2008).....	25
Figure 3.2 Lamia's Gardens: Plan of the 1873-1876 findings, between Foscolo street, Emanuele Filiberto Street and Dante Square (Lanciani, 1986).....	28
Figure 3.3 Lamia's Gardens: Topographical plan with indication of the main excavations from 1873 to 2009 (Barbera et al., 2010).....	31
Figure 4.1 Seven pill moulds with the mounted samples.....	37
Figure 4.2 Scanning Electron Microscope FEI-QUANTA 400 (SEM-EDAX).....	37
Figure 4.3 Electron microprobe CAMECA SX50.....	38
Figure 5.1 Image of sample No.1 taken by OM.....	41
Figure 5.2 Image of sample No.2 taken by OM.....	41
Figure 5.3 Image of sample No.3 taken by OM.....	42
Figure 5.4 Image of sample No.4 taken by OM.....	42
Figure 5.5 Image of sample No.5 taken by OM.....	43
Figure 5.6 Image of sample No.6 taken by OM.....	43
Figure 5.7 Image of sample No.7 taken by OM.....	44
Figure 5.8 Image of sample No.8 taken by OM.....	44
Figure 5.9 Image of sample No.9 taken by OM.....	45
Figure 5.10 Image of sample No.10 taken by OM.....	45
Figure 5.11 Image of sample No.11 taken by OM.....	45
Figure 5.12 Image of sample No.12 taken by OM.....	46
Figure 5.13 Image of sample No.13 taken by OM.....	46
Figure 5.14 Image of sample No.14 taken by OM.....	47
Figure 5.15 Image of sample No.15 taken by OM.....	47
Figure 5.16 Image of sample No.16 taken by OM.....	48
Figure 5.17 Image of sample No.17 taken by OM.....	48
Figure 5.18 Image of sample No.18 taken by OM.....	49
Figure 5.19 Image of sample No.19 taken by OM.....	49
Figure 5.20 Image of sample No.20 taken by OM.....	50
Figure 5.21 SEM image of sample No.2 and its respective bulk spectrum taken by EDS as an example of glass with a tin and calcium-rich opacifier.....	51
Figure 5.22 SEM image of sample No.3 and its respective bulk spectrum taken by EDS as an example of glass with high concentration of lead and copper.....	51
Figure 5.23 SEM image of sample No.3 as an example of big circular bubbles.....	52
Figure 5.24 SEM image of sample No.5 and its respective bulk spectrum taken by EDS as an example of low levels of sodium.....	52
Figure 5.25 SEM image of sample No.10 as an example of elongated bubbles.....	53
Figure 5.26 SEM image of a titanium and iron-rich inclusion from sample No.12 and its respective spectrum taken by EDS.....	54
Figure 5.27 SEM image of sample No.13 as an example of homogeneous glass with a few bubbles.....	54
Figure 5.28 SEM image of sample No.17 as an example of extensive superficial deterioration.....	55
Figure 5.29 SEM image of an aluminum, iron and potassium-rich inclusion from sample No.19 and its respective spectrum taken by EDS.....	56
Figure 5.30 Chondrite-normalized (McDonough and Sun, 1995) trace element composition of the glass samples analyzed by LA-ICP-MS.....	59
Figure 6.1 Ternary diagram of the normalized Na <sub>2</sub> O, MgO+K <sub>2</sub> O and CaO contents of all the glass samples analyzed by EMPA (Gratuze and Janssens, 2004).....	63

Figure 6.2 K <sub>2</sub> O vs MgO concentration (wt%) for all the analyzed samples by EMPA.....	64
Figure 6.3 K <sub>2</sub> O vs MgO concentration (wt%) for the red glass (5) analyzed by EMPA .....	65
Figure 6.4 Ba vs MnO concentration (ppm/wt%) for all the samples, as collected by LA-ICP-MS and EMPA respectively .....	69
Figure 6.5 Plot of the elements related to recycling analyzed by LA-ICP-MS .....	71
Figure 6.6 Ba vs Sr (ppm) for all the analyzed samples by LA-ICP-MS.....	73
Figure 6.7 TiO <sub>2</sub> /Al <sub>2</sub> O <sub>3</sub> vs Al <sub>2</sub> O <sub>3</sub> /SiO <sub>2</sub> (wt%) for all the analyzed samples by EMPA (Schibille et al., 2017) .....	74
Figure 6.8 Concentration ratio of Ce/La (ppm) vs Zr/SiO <sub>2</sub> (ppm/wt%) for all the samples analyzed by EMPA and LA-ICP-MS (compared to Ceglia et al., 2019) .....	74
Figure 6.9 Concentration ratio of Sr/CaO vs Zr/SiO <sub>2</sub> (ppm/wt%) for all the samples analyzed by EMPA and LA-ICP-MS (compared to Ceglia et al., 2019) .....	75

## List of Tables

Table 4.1 Summary of the basic characteristics of the glass samples .....	33
Table 4.2 Continued from previous page .....	34
Table 4.3 Continued from previous page .....	35
Table 4.4 Continued from previous page .....	36
Table 4.5 References used for the quantitative analysis of the chemical elements.....	38
Table 4.6 Operating conditions of LA-ICP-MS.....	39
Table 4.7 Operating conditions of LA-ICP-MS.....	39
Table 4.8 Isotopes analyzed by LA-ICP-MS and their dwell times .....	40
Table 5.1 Major oxides (in wt%) measured by EMPA .....	57
Table 5.2 Major oxides (in wt%) measured by EMPA .....	58
Table 5.3 Minor and trace elements (in ppm) measured by LA-ICP-MS.....	60
Table 5.4 Continued from previous page .....	61

# 1. Introduction

## 1.1. Background of Study

Ancient glass was composed of three main ingredients, namely a source of silica in the form of sand or quartz pebbles as a network former, an alkali, added as flux to reduce the melting temperature of silica, and lime, used as a stabilizer. More raw materials were added to produce a specific colour or opacity (Grose, 1989; Ganio et al., 2012; Henderson, 2013). Glass objects have been found sporadically since the 3rd millennium BC (Grose, 1989; Slough, 2005; Henderson, 2013), but their widespread use started during the Roman Empire (Grose, 1989; Stern, 1999; 2012; Ganio et al., 2012; Henderson 2013). Thus, glass fragments are frequently found in Roman archaeological excavations. Among the glass finds, architectonic glass is a big category, as glass started to be used extensively for decoration purposes from the 1st century AD onwards. Architectonic glass includes mosaic *tesserae*, *opus sectile*, inlays, twisted rods, revetment plaques and window panels (Cosyns, 2006; Boschetti, 2011).

Archaeometric studies conducted on Roman glass have given useful information on glass-making techniques, provenance of raw materials and trade routes (Degryse et al., 2014; Bugoi et al., 2018). It is strongly supported that raw glass was produced in a limited number of primary workshops using local raw materials in Eastern Mediterranean and later it was distributed in secondary workshops found in many locations, where glass objects were produced (Freestone et al., 2000; 2005)

The research for the early Roman period (1st-3rd century AD) is limited. Most of these studies point to a possible Eastern Mediterranean provenance of the glass, but silica sources seem to be different than in later glass (Nenna et al., 1997; Ganio et al., 2012; Gallo et al., 2015).

Based on differences in aluminium, lime and iron oxide concentrations, it is suggested that late Roman glass has been produced either on the Syro-Palestinian coast (Levantine I, Levantine II) or in Egypt (Egypt I, Egypt II, HIMT) (Nenna, 1998; Freestone et al., 2000; 2005; Tal et al., 2004; Paynter, 2006). These categories are further sub-divided on grounds of minor and trace elements (Picon and Vichy, 2003; Foster and Jackson, 2010).

Regardless of the increasing volume of analytical data on glass during the last decades, there are only a few analyses on architectonic glass. Several studies have been conducted only on glass mosaic *tesserae* (Arletti et al., 2006; 2008; Boschetti, 2011; Ricciardi, 2009; Verità and Santopadre, 2015; Maltoni and Silvestri, 2018) but other types of architectonic glass are rarely examined. For instance, there are studies on Roman *opus sectile* fragments from only five locations, namely 100 panels found in the port of Kenchreai (Brill, 1976), a



panel in *opus sectile*, known as Thomas panel, probably found in Faiyum (Brill and Whitehouse, 1988), a *domus* near Ostia (Verità et al., 2008), a villa in Faragola (Santagostino Barbone et al., 2008; Gliozzo et al., 2010) and the Villa of Lucius Verus in Rome (Verità et al., 2013; Bandiera et al., 2019; Bandiera et al., 2020; Tesser et al., 2020) covering a limited range of chronology from the second half of the 2nd to the 4th century AD. These studies focused on (de)colourants, opacifiers and provenance of the raw materials.

## 1.2. Object of Study

The present thesis presents an archaeometric study concerning the morphological and chemical characterization of glass samples found in Rome. Particularly, the glass selected for the analysis was excavated in Lamia's Gardens, which is located on the southern part of the Esquiline hill. They are fragments of architectonic glass of various colours (red, orange, yellow, green, blue, white, brown and black) including fragments of *opus sectile*, inlays, revetment plaques and twisted rods. They were excavated during the last intervention of the site between 2006 and 2009, covering the area between the square Vittorio Emanuele II, the street Emanuele Filiberto, and the street Conte Verde. The studied material could be dated to the second half of the 1st century or the 2nd century AD.

The glass samples have been examined through a multi-analytical approach including the use of Optical Microscopy (OM), Scanning Electron Microscopy coupled with Energy Dispersive X-ray Spectroscopy (SEM-EDS), Electron Microprobe Analysis (EMPA) and Laser Ablation Inductively Coupled Plasma Mass Spectrometry (LA-ICP-MS). The scientific research was designed to shed light on glass-making production and provenance of the raw materials.

The archaeometric study of the material was undertaken at Sapienza University of Rome, Italy and at the HERCULES Laboratory of the University of Évora, Portugal.

## 1.3. Research aim

The archaeometric study on the glass fragments excavated in Lamia's Gardens aims to discuss the glass-making technique and provenance of the raw materials of early Roman architectonic glass. The research methodology was designed using a multi-analytical approach to collect a series of complementary data relevant to the study.

This research work comprises three independent and interconnected major goals. The initial goal was to obtain data regarding the morphology of the glass fragments and their elemental composition in terms of major, minor and

trace elements. The interpretation of these data contributes to assessing the technological choices made by the glassworkers. The second major goal was identifying the raw materials used with special attention to (de)colourants and opacifiers. Lastly, the potential sources of the raw materials used for the production of glass were examined to suggest the location of the primary production centres.

The analysis of the glass fragments from Lamia's Gardens is considered important, as the findings of the recent excavation have been barely studied until now. Therefore, there is the need for analyzing the excavated artifacts and better reconstruct the history of the site. Moreover, architectonic glass, except mosaic *tesserae*, is rarely studied. For that reason, the present study will provide valuable information about the method of production of architectonic glass and subsequently the technological level achieved in the 1st-2nd century AD. It is worth mentioning that the glass fragments in this study are the earliest architectonic glass to be analyzed until now.

#### 1.4. Overview of the chapters

Initially, Chapter 1 intends to give an introduction to the thesis. This is achieved through a summary of the state of the art for the production of Roman glass and of architectonic glass in particular. Moreover, the object, the methods and the aims of the research are presented shortly.

Afterwards, Chapter 2 contains general information about glass and glass making. The scope of the chapter is to define glass and to describe its main constituents with a focus on their role in glass formation. Moreover, the distinction between primary and secondary workshops will be addressed. Additionally, the history of glassmaking and the techniques used for the production of glass objects from the beginning of glass production until Roman times, with a special mention to architectonic glass will be briefly addressed.

A detailed description of the history of Lamia's Gardens and the history of research will be given in Chapter 3. This section will indicate the importance of the site and the different phases of its construction.

Chapter 4 will provide details about the glass fragments analysed in terms of colour, use, date and exact location, where they were excavated. Furthermore, information about sample preparation and the methods used for their analysis along with the experimental setup of the instruments will be given.

The results of the analysis will be presented in Chapter 5. The results of each technique will be provided separately. Especially for OM and SEM-EDS, the observation for each sample will be independently described, whereas the chemical analyses performed by EMPA and LA-ICP-MS will be also compared.

Chapter 6 will give an interpretation of the results. It is divided into two main sub-chapters. The first will focus on glass-making technology discussing primary raw materials, (de)colouring and opacifying agents that gave glass its particular appearance. The second sub-chapter will focus on the provenance of the raw materials used.

Finally, the thesis will end with Chapter 7 providing the final remarks.

## 2. Glass

### 2.1. Definition

All types of glass can be described as “an amorphous solid completely lacking in long-range, periodic atomic structure, and exhibiting a region of glass transformation behaviour” (Shelby, 2005).

Particularly for ancient glass, the main constituent is silica ( $\text{SiO}_2$ ), which is the network former. As the melting point of pure silica is  $1700^\circ\text{C}$ , which was unattainable by ancient craftsmen, another “ingredient” was added to the batch to reduce its melting point – the flux. The most common fluxes in antiquity were soda ( $\text{Na}_2\text{O}$ ) and potassium ( $\text{K}_2\text{O}$ ). Both can lower the melting point of glass to around  $1150^\circ\text{C}$  (Matson, 1951; Shelby, 2005). Additionally, the melting temperature was lowered by adding recycled glass, from the Flavian period onwards (Stern, 1999; Silvestri et al., 2008). Lastly, a glass stabilizer, usually lime ( $\text{CaO}$ ), was employed (Hodges, 1981). This constituent improved the durability of glass. Lime made glass more resistant in terms of its chemical properties and it limits the tendency for corrosion, decay and opacification. Nevertheless, if the amount of calcium exceeded a certain upper limit, glass tended to devitrification. This phenomenon could be avoided by adding alumina ( $\text{Al}_2\text{O}_3$ ) or magnesia ( $\text{MgO}$ ) to the batch, which also act as stabilizers (Degryse, 2014). Glass also consisted of other raw materials, which changed its optical properties, like colour or opacity. For example, copper was added to produce blue, turquoise, green or red glass depending on the furnace atmosphere (Henderson, 2000; Bandiera et al., 2019).

There are many recipes to produce glass, each involving different proportions of the main raw materials and resulting in glass with different chemical and physical properties. Therefore, the composition of glass is distinct in terms of time and space (Brill and Cahill, 1988).

### 2.2. Raw Materials

#### 2.2.1. Network former

Ancient glass is composed of approximately 65-70% silica ( $\text{Si}_2\text{O}$ ). Silica is a polymorph that has three principal forms: quartz, tridymite and cristobalite. Among them, quartz is the most common and the one used to produce glass (Henderson, 2013). Sources of silica for glassmaking could be pebbles, riverine and coastal sand or inland geological deposits (Henderson, 2013). Quartz pebbles are a pure source of silica, whereas sand contains many undesirable heavy minerals. Common minerals found in the sand are feldspar, magnetite, ilmenite and silicates (Henderson, 2000). Moreover, sand could include shell fragments that introduce the necessary amount of lime into the batch (Freestone et al., 2005).

### 2.2.2. Fluxes

The flux is added to the glass to lower the melting point of silica. More precisely, silicon atoms bonded to oxygen form a strong and rigid network of silica tetrahedral, which can be melted at  $\sim 1700$  °C. The addition of flux into the batch disrupts the continuity of the glass network, inducing a partial network opening so that the structure becomes weaker. As a result, melting point and viscosity of glass decrease, whereas its thermal expansion coefficient and crystallization tendency increase (Shelby, 2005; Degryse et al., 2014). The fluxes used in ancient times were mainly potassium ( $K_2O$ ) and soda ( $Na_2O$ ), which came from two sources: plant or wood ashes and natron, respectively (Grose 1989; Henderson, 2013). Lead oxide ( $PbO$ ) could also act as a flux (Shelby, 2005; Degryse et al., 2014).

The plants used for glassmaking were chosen according to their amount of sodium and perhaps their amount of calcium (Henderson, 2013). It has been proposed that the ashes of halophytic plants of the *Chenopodiaceae* family were employed (Henderson, 2013). According to Flowers (1986), “halophytes are plants adapted to live in a saline environment”. As their ash contains adequate quantities of sodium carbonate, they are suitable for glass making. This salt is responsible for reducing the melting point of silica from  $\sim 1700$  °C to  $\sim 1150$  °C (Matson, 1951; Henderson, 2013). In medieval times, wood ashes were also used as a source of alkali to produce the so-called forest glass (Freestone, 1991). Glass made with plant or wood ashes is easily recognizable by the relatively low concentration of sodium ( $Na_2O$  12.7-14 wt%) and relatively high content of potassium and magnesium (both 2.3-2.5 wt%) together with phosphorus oxides ( $P_2O_5$  0.7-1 wt%) (Sayre and Smith, 1961).

The mineral natron ( $Na_2CO_3 \cdot 10H_2O$ ) started to be used in glassmaking around the 10th century BC and it replaced plant ashes gradually. It was the main alkali source till 800 AD in the West and Middle East (Henderson, 1985; Freestone et al., 2000). Natron is a pure source of sodium carbonate, and it could contain a few minor and trace elements (Degryse and Shortland, 2020). It has been proven that it mainly came from Wadi Natrum, a zone with several small, stagnant lakes between Cairo and Alexandria, in Egypt (Henderson, 1985). The minerals that occur there are formed seasonally as water evaporates from the surface of alkali-rich soils. Natron was known to the Egyptians as early as the Fourth Egyptian Dynasty (2575-2465 BC), as it was widely used in mummification, medical preparations, and the whitening of linen (Ignatiadou et al., 2004; Saguí, 2010). Other locations have been also studied as possible source of natron, such as Lake Pikrolimni in Greece, but there is no strong evidence to support its use in glass production (Ignatiadou, 2002; Ignatiadou et al., 2004).

Natron glass is recognizable by a high content of sodium ( $\text{Na}_2\text{O}$  17-21 wt%) and low concentration of potassium ( $\text{K}_2\text{O}$  0.5-0.7 wt%), magnesium ( $\text{MgO}$  0.6-0.7 wt%) and phosphorus oxide ( $\text{P}_2\text{O}_5$  0.1 wt%) (Sayre and Smith, 1961).

### 2.2.3. Stabilizers

Alumina and alkaline earth, namely calcium and magnesium oxides, act as stabilizers of the glass (Janssens, 2013). They are added into the glass network by bonding to the atoms of oxygen, which results in breaking down silicon tetrahedra. They could be added to the batch through heavy minerals present in the sand or non-purified plant ashes (Shelby, 2005; Janssens, 2013). Additionally, calcium could derive from shell fragments included in the sand (Freestone et al., 2005). If plant ash or sand did not have the required amount of calcium, it would have been added separately as a third primary raw material. Further evidence for the intentional addition of lime in the glass batch comes from Pliny, as he refers to the addition of lustrous stones and shells to the glass (Pliny, *Natural History*, XXXVI). From the medieval period onwards, bones and dolomitic limestone have been also employed occasionally as sources of calcium (Grose, 1989; Henderson, 2013).

### 2.2.4. Fining agents

The chemical compounds added to the melt for facilitating the removal of air bubbles are called fining agents. They release large quantities of gases, which subsequently form large bubbles. These bubbles rise to the surface of the melt also carrying smaller bubbles. Moreover, some fining agents provoke the absorption of oxygen from the bubbles reducing their size (Shelby, 2005). Antimony and arsenic in a range between 0.1 and 1 wt% are the most common fining agents. Sulphates, nitrates, halides and the oxides of a few polyvalent cations could also act as fining agents (Shelby, 2005). Although their use is widespread in the modern glass industry, only antimony could have that function in ancient glass (Henderson, 1985; Brill and Cahill, 1988; Jackson, 2005).

### 2.2.5. Colourants and decolourants

It is often suggested that the first glasses were created to imitate precious stones so that the colour of the new material was a very important characteristic (Grose, 1989; Rutten et al., 2009; Henderson, 2013; Tesser et al., 2020). Heavy minerals in the raw materials, and particularly the ones containing iron oxides, gave the glass a natural green-blue colour. The production of a specific glass colour depends on a range of complex factors including the preparation of the glass batch, the colourants used, the atmosphere in the furnace and the maximum temperature achieved (Hodges, 1981; Henderson, 2000). Therefore, ancient glassmakers had to be

able to carefully choose the raw materials and to precisely control the firing conditions. Colouring agents were added in the primary glassmaking process or in an intermediate stage, before glass working (Henderson, 1985; 1989; 2000).

The most common colour in early glass was blue as a way for imitating *lapis lazuli*, a stone that was considered to have health-giving properties and very popular in the Bronze Age. The deep blue colour was achieved by the addition of a cobalt source (CoO). As it is a powerful colourant, a small amount (as small as 0.02%, present as  $\text{Co}^{2+}$ ), was enough to impart such deep blue colour (Arletti et al., 2006; Henderson, 2013).

Moreover, another common colouring agent of glass was copper. It was used to produce pale blue or red glass (Henderson, 2000; Bandiera et al., 2019). The production of red glass has drawn the attention of many scholars, as it seems to have been produced with plant ash even in Roman times (Henderson, 1991; Santagostino Barbone et al., 2008; Gliozzo et al., 2010; Bandiera et al., 2020). It is considered that the addition of plant ash and charcoal in the glass melt would create more easily the necessary reducing conditions for the production of the reduced form of copper ( $\text{Cu}^+$ ) for the red glass.

Although the colour was an important characteristic of glass for many centuries, the production of colourless glass was also known from the 2nd millennium BC. It was especially popular in the Hellenistic period, from the 6th century until the 2nd century BC, in the Roman period, from 70 AD onwards, and in the 14th century (Sayre and Smith, 1961; Henderson, 2013). It could be produced either by using a pure source of silica with low levels of iron or by adding antimony trioxide ( $\text{Sb}_2\text{O}_3$ ) or manganese oxide ( $\text{MnO}_2$ ) to the batch to neutralize the green-blue colour (Brill and Cahill, 1988).

Antimony trioxide was the main decolourant in the Hellenistic period, whereas manganese oxide was preferred from the 2nd century BC onwards (Freestone, 1991; Henderson, 2000). It is worth mentioning that manganese could be used either as decolourant or as colourant to produce purple or yellow glass.

#### 2.2.6. Opacifiers

The manufacture of opaque glass could be achieved in many ways (Henderson, 1985; 2000; Freestone, 1987; Tite and Shortland, 2008; Rutten et al., 2009). Specifically, opaque glass could be induced by the presence of insoluble particles, silica crystals or gas bubbles, as visible light is reflected by them (Henderson, 2013).

Moreover, the intentional addition of materials called opacifiers could produce opaque glass. For example, calcium antimonate ( $\text{Ca}_2\text{Sb}_2\text{O}_7$  and  $\text{Ca}_2\text{Sb}_2\text{O}_6$ ) and later tin oxide ( $\text{SnO}_2$ , cassiterite) were the main opacifiers for



white glass (Lahlil et al., 2008). This glass is often combined with copper, manganese, or cobalt to produce their respective opaque colours. Yellow and green opaque glasses were produced by adding either lead antimonate ( $\text{Pb}_2\text{Sb}_2\text{O}_7$ ) or lead stannate ( $\text{Pb}_2\text{SnO}_4$ ) (Wainwright et al., 1986; Verità et al., 2013). Lastly, opaque brownish-red glass was made by the addition of a reduced copper source ( $\text{Cu}_2\text{O}$ ) (Bandiera et al., 2020).

### 2.3. Production of glass

The production of glass involves many different steps, including the selection of raw materials, the making of the raw glass, the formation of the glass objects and the annealing process. These stages are usually divided into two categories, namely primary and secondary production (Brill and Cahill, 1988). There is a big debate about if these two stages happened at the same location in antiquity.

The primary production consists of the selection of raw materials and their melting, possibly involving fritting. Fritting is a process carried out in special ovens at relatively low temperatures of about 600 °C. It is stopped before glass begins to form resulting in a grey friable crystalline material. The main aim of fritting is the purification of the raw materials by breaking down the former salts such as carbonates, sulphides and sulphates and thereby producing gaseous carbon monoxide, carbon dioxide and sulphur dioxide. The release of gases from the melt would produce glass with fewer bubbles. Moreover, fritting results in the promotion of the complete fusion of the glass raw materials and the reduction of the volume of the raw glass (Henderson, 2013). The result of primary production is raw glass in the form of ingots or chunks, which can be transported to secondary production centres. Primary centres could be recognised by the discovery of overheated frit and fritting ovens, the shape and the size of the glass furnaces, *i.e.*, large tank furnaces (Henderson, 2000). Nevertheless, this furnace could be also used for the reheating of glass, so that it was useful for the production of glass objects. The archaeological findings for primary workshops are rare and difficult to identify, as the structures were destroyed after each firing to extract the raw glass and they could be also used for secondary production (Gorin-Rosen, 2000). Currently, there is only some evidence for glass making for the Bronze Age and from the Roman period onwards (Henderson, 2000; Conte et al., 2014).

This gap is partially filled with ancient literary sources and scientific analysis. On one hand, ancient sources, such as the cuneiform tablets from King Ashurbanipal's (669-631 BC) library or the work of Roman writers such as Tacitus (Tacitus, History, V.7), Pliny (Pliny, Natural History, XXXVI) and Strabo (Strabo, Geography, XVI), describe raw materials and production methods. On the other hand, scientific analysis of the raw materials can provide evidence of their provenance. Particularly for the silica source, it is



believed that the sand used for the production of raw glass was located in the vicinity of the glass workshop. Therefore, a provenance study on sand could also indicate the location of glass manufacture (Degryse et al., 2014).

The secondary glass production consisted in working the raw glass in many ways. The process included melting of the raw glass, moulding, slumping, blowing, shaping and decorating. It could be done by traveller artisans, who transported their tools and the raw material according to the demand. Such examples have been found next to sanctuaries in Olympia, Ain Manawir, Gumaiyama and Tebtynis, cities where glassworkers remained only the necessary time to complete the glass objects needed for the sanctuary (Nenna, 1998). Glassmaking could be also done in more permanent structures, which are identified in archaeological contexts by the recovery of glass furnaces, annealing ovens, moulds, crucibles, pulls of glass and tools such as blowing pipes and pontil rods. The furnaces for glassmaking were usually smaller and built in a precarious way, as they were used for short periods. They could also contain a chamber for annealing (Henderson, 2013). More secondary centres have been identified, mainly inside the cities, where there were enough customers to buy their products.

## 2.4. History of glass production and glass making techniques

### 2.4.1. Early glass production

Although the information about the early production of glass is scarce, it is considered that it was invented in the Middle East around 2500 BC. Specifically, it has been suggested that it was probably firstly made in Iraq or northern Syria (Slough, 2005; Henderson, 2013). The discovery of early glass is limited to a few sites and usually not well dated. For example, some of the earliest glass objects found are: one bead in Tell Judedeh, Syria, dated earlier than the 3rd millennium BC (Braidwood, 1960) and a glass pin from Nuzi, Iraq, dated to 2350-2150 BC (Starr, 1939).

In the beginning, raw glass was made from silica and plant ash, and it was fused in small crucibles. Then, it was cold-worked by cutting, grinding and polishing into a variety of colourful small artefacts, like beads, seals, rods and inlays. Vessels started to be produced only in the late 16th/15th century BC. Based on their geographical distribution, Nolte (1968) suggested that their invention was made in North Mesopotamia.

In the 16th century BC, new working techniques were introduced in Mesopotamia (Barag, 1985). Specifically, vessels were more often made with a core-forming method, meaning that a core in the shape of the desired vessel was manufactured from a mixture of clay, mud and possibly sand, usually with an organic binder. The core was then covered with hot glass. The vessel was finished by rolling it on a flat stone. After decoration, the core was

removed. This is the most popular technique until the Hellenistic period. A similar technique is rod-forming, in which a metal rod was added to the core. This method was preferred for long and narrow containers and many small objects (Grose, 1989).

Casting was another glassmaking technique that started to be used in the 16th century BC. This technique involved the use of moulds for the manufacture of vessels and objects. An interesting example of casting is mosaic glass that started to be produced already from the 15th century BC. Mosaic glass was prepared by melting preformed canes inside a mould. Glass pieces were usually arranged in a geometric pattern resulting in objects with elaborate designs (Grose, 1989; Henderson, 2013).

In this period, glassmaking also started in Egypt. It has been suggested that glass production spread in Egypt when Thutmose III (1493-1436 BC) returned to Egypt from his military campaigns in Palestine and Syria with local glassmakers (Harden, 1968). The earliest possible primary production centre was discovered in Egypt, particularly in Tell el-Amarna and it is dated to the reign of Akhenaten (1353-1337 BC) (Nicholson, 2007). Although there is evidence for glass fusion in Egypt, many scholars support the importation of most of the raw materials from the Middle East (Oppenheim, 1973).

At the end of the 13th century BC, the main centres of glass production collapsed. As a result, archaeological remains from the following period (1200 to 900 BC) are scarce (Barag, 1985). The only significant amount of glass assemblage comes from the site of Frattesina in northern Italy, where a glass industry probably existed in the 11th-9th century BC (Bellintani, 1997).

During the 9th century BC, the first signs of revival of glass production manifested in Phoenicia and Syria. Nevertheless, most of the glass objects, including vessels and a significant number of plaques and inlays used for decorative purposes and found in Mesopotamia and Egypt, were dated to the 8th century BC (Grose, 1989). The same raw materials and production methods as in the Bronze Age continued to be used. This glass industry also collapsed in the late 7th century BC, when the Assyrian kingdom was destroyed, and the Phoenician coast was devastated. Some of these techniques, such as casting, were revived in the 5th century BC by the Persians.

#### 2.4.2. Glass production during the Hellenistic period

Even though the evidence for glass production during the Classical period is scarce, there is a noticeable renaissance of glass production in the Hellenistic period. As there is no adequate archaeological evidence about glass production centres, the proposed locations are Rhodes (Triantafyllidis, 2003), Macedonia (Ignatiadou et al., 2004), southern Italy (Grose, 1989), Alexandria

(Barag, 1985; Grose, 1989) and the Syro-Palestinian coast (Jackson-Tal, 2004). The sole archaeological remains of glass production centres were found in Bosra, southern Syria, and in Beirut, Israel (Dussart, 1998; Kowatli et al., 2008). The Hellenistic glass industry was deeply influenced by Persian casting, so cast tableware was very popular until the 3rd century BC. In the 3rd and 2nd century BC, a more distinct Hellenistic glass production was created. It was characterized by the use of highly coloured glass and a variety of techniques, like sagging and casting. It is also important to highlight the increase of the scale of production in the middle and late Hellenistic period. This increase is probably due to an increase in population and in long-distance trade, which consequently created a greater demand for glass objects (Henderson, 2013).

#### 2.4.3. Roman glass production

It is often highlighted that late Hellenistic industries laid the foundation for Roman glass production. In fact, in the early Roman period, glass was produced according to the Hellenistic tradition in terms of raw materials and methods of production (Grose, 1989; Aerts et al., 2003). Especially for the raw materials, the analysis of the chemical composition of the early Roman glass showed that it was fused with the same raw materials and colourants of Hellenistic glass, probably from the Syro-Palestinian coast.

A radical change happened in glass production in the mid-1st century BC, when glassblowing was invented (Grose, 1989; Stern, 1999; 2012; Henderson 2013). Being simple and quick, this production method permitted the mass production of glass objects. Indeed, the artisan could produce up to 100 vessels per day. For the first time in history, glass became available to a big part of the population (Stern, 1999).

The earliest archaeological evidence for glassblowing is found in a ritual bath in the Jewish quarter of Jerusalem old city from around 50 BC (Israeli, 2005). Glassblowing expanded quickly in all the Mediterranean and became very common from the second half of the 1st century BC onwards. Therefore, researchers believe that glassblowing was invented on the Syro-Palestinian coast, but it was further developed in Italy (Stern, 1999).

The glass blowing technique produced objects using raw glass in a viscous state. The glassmaker used a hollow or metal pipe to take a gather of glass. Then, he blew into the open end of the pipe, expanding the glass into a bubble. While still hot, the glass could be transformed in various sizes and shapes (Stern, 2012). The invention of the closed heat chambers furnace and of the iron pipe incredibly aid the development of the method, as this type of furnace could heat the objects evenly in high temperatures and iron could endure high temperatures (Stern, 2012). The technique was further refined

with the use of moulds in the second quarter of the 1st century AD (Grose, 1989).

Specifically for Italy, an increase in production and use is attested in literary sources and archaeological findings from the Augustan period onwards (Grose, 1989). The significance of glass is even evident in the social prestige of the glassmakers. It seems that they were so praised for their abilities, that they started signing vessels using their name and the Greek verb *epoiesen/epoie*, which means *to make*. The most common names attested are Ennion, Aristeas, Iason, Meges and Neikais (Stern, 1999; Saguí, 2010).

The 1st century AD was the century of experimentation in Roman glassmaking. An increase both in the number of glass objects and the functions they served is attested (Grose 1989). For instance, a purely Roman invention was cameo glass (Bimson and Freestone, 1983; Saguí, 2010). It is considered that it was invented during the Augustan era. Although there are also some findings from the Claudio-Julian period, its production is limited in time and space. It was used to form exclusively luxurious objects, as it was a labour-intensive technique. They consisted of a blue, or more rarely a purple background, on top of which the decoration was carved on white glass.

The quick development of the Roman glass industry is usually attributed to three factors (Grose, 1989). Particularly, the increase in trade provided the necessary conditions for glass to reach all parts of the empire. Furthermore, it seems that trade and the relatively easy movement of people and products also resulted in a rapid spread of knowledge on glassmaking in the empire. Lastly, the ability of the Romans to assimilate and improve previous glassmaking traditions enabled them to experiment and to produce a wide variety of objects.

It needs to be mentioned that the glass industry continued to develop evenly in the 2nd and 3rd centuries AD, but there was a drastic change in the second half of the 4th century in terms of stylistic characteristics, colour and composition. Specifically, the most common tableware is produced in a dark green or brown colour and the concentration of chemical elements such as iron, manganese, titanium, copper, zinc and zirconium is higher. This is usually explained by using recycled glass or different raw materials. Moreover, Price (2000) highlights that quicker and simpler production methods are employed in this period.

Chemical analysis of Roman glass has shown that its composition is very homogeneous regardless of place and time of manufacture (Sayre and Smith, 1961; Nenna et al., 1997; Aerts et al., 2000). This is particularly true for major elements, as Roman glass consists of approximately 66-72% SiO<sub>2</sub>, 16-18% Na<sub>2</sub>O and 6-8% CaO. Slight differences in composition are usually attributed to the use of different colourants. This homogeneity has been explained by the

use of the same raw materials. Particularly, it is suggested that the use of a pure source of sand and natron resulted in a homogeneous glass with low levels of heavy minerals (Sanderson et al., 1984). Other scholars suggested that the compositional stability could also be owed to a strict recipe (Lemke, 1998) or the precise control of the manufacturing process (Rehren, 2000).

As for the organization of the primary and secondary production centres, there are two models suggested based on literary sources, archaeological evidence and chemical analysis of the findings. On one hand, some scholars suggest the local production of raw glass according to the local demand, which would result in many distinct chemical compositions of the glass (Price, 2005; Paynter, 2006). On the other hand, the centralized model suggests that the primary glass production happened in a limited number of centres and then the glass was exported to small secondary workshops across the Empire (Freestone et al., 2005). If this model is true, one could expect that the chemical composition of glass would be more homogenous (Paynter, 2006). The most favoured model is the second one, suggesting that raw glass was produced, mainly, in Egypt and the Levant and then transported in secondary workshops across the empire (Freestone et al., 2000; 2005).

Even ancient authors usually distinguished the location of the raw materials and the fusion of glass. For example, Strabo (Strabo, Geography, XVI) refers to three main production centres, namely Syro-Palestine, Alexandria and Italy, whereas Pliny (Pliny, Natural History, XXXVI) to the Middle East, Italy, Gaul and Spain.

As for archaeological evidence, findings for the early Roman glass production centres are scarce (Paynter, 2006), but there is more evidence for the late period, as several tank furnaces have been found mainly in Egypt and the Levant (Gorin-Rosen, 2000; Nenna, 2000; Freestone et al., 2000; Nenna et al., 2005; Kowatli et al., 2008). The most mentioned discovery is the archaeological site of Bet Eli'ezer in Israel dated to the 8th century AD, where the remains of 17 rectangular furnaces have been found (Freestone et al., 2000; 2005; Gorin-Rosen, 2000). Moreover, four tank furnaces dated to the 6th-7th century AD have been found in Apollonia, in Israel (Gorin-Rosen, 2000; Tal et al., 2004; Freestone et al., 2000; 2005). Regarding Egypt, glass furnaces were found close to Wadi Natrun dating to the 1st-2nd century AD (Nenna, 2000; Nenna et al., 2005) and on the shores of Lake Maryut, close to Alexandria, dating from the imperial era until the 8th century AD (Nenna, 2000). Hence, a concentration of workshops nearby the silica source, *i.e.*, the mouth of River Belus, or close to the natron source, *i.e.*, Wadi Natrun (Freestone et al., 2000; Nenna, 2000), is evident.

Nevertheless, archaeological evidence for glass production has been also found in other parts of the empire. Specifically, tank furnaces have been

found in Britain (Shepherd and Heyworth, 1991), France (Rebourg, 1989), Germany (Wedepohl, 2000) and Switzerland (Morel et al., 1991). These furnaces suggest the existence of many small production centres probably operating for short periods of time.

Archaeological findings in shipwrecks, including a big amount of raw glass, are considered important, as they are proof of the transport of glass throughout the Mediterranean Sea. As examples, raw glass ingots and cullet have been found in the shipwreck "Ouest-Embiez 1", close to the coast of France (Fontaine and Foy, 2007) and "Iulia Felix" in the Adriatic Sea (Silvestri et al., 2008).

Despite the scarce evidence for primary production centres, secondary workshops are more prolific all over the Empire (Degryse et al., 2014). For example, there are more than 70 workshops excavated in France (Price, 2005) and more than 20 in Britain (Jackson et al., 2003; Price, 2005; Paynter, 2006). Although the evidence for secondary workshops in West Europe surpasses the East (Stern, 2002), glass working is also attested in the latter. The most mentioned workshop in the East is located at Jalame, in Palestine, dated to the late 4th century AD (Brill and Cahill, 1988).

Lastly, the chemical analysis of glass has demonstrated some distinguishable compositional types. Specifically for the Roman period, the glass is considered homogeneous between the 1st and the 3rd century AD. Indicatively, Nenna et al. (1997) calculated the mean composition of the Early Roman glass as 69.54% SiO<sub>2</sub>, 16.63% Na<sub>2</sub>O, 0.75% K<sub>2</sub>O, 7.48% CaO, and 0.59% MgO. The differences are attributed to the use of different colourants.

From the 4th century onwards, the composition of Roman glass is more diversified. Firstly, there is a distinction between Egyptian and Levantine glass. Egyptian glass is characterized by a high concentration of aluminium (3-4.5%) and a low level of calcium oxide (3-4%) (Gratuze and Barrandon, 1990; Freestone, 1994; Nenna et al., 1997). This type of glass was in use until the 8th century, but the beginning of its production is unsure (Gratuze and Barrandon, 1990). On the other hand, glass from the Levant dated to the late Roman period is characterized by a relatively high level of calcium oxide (8-9%) and a low level of alumina (2.5-3%) (Freestone et al., 2000). Lastly, a glass type known as HIMT, *i.e.*, high iron, manganese and titanium, is used from the late 4th century onwards (Freestone, 1994; Freestone et al., 2005). Specifically, this type of glass is distinguishable due to the unusually high amount of iron (2-3%), manganese (2-3%) and titanium (0.5-1%). Egypt has been proposed as the location of the production centre for HIMT glass (Freestone et al., 2005). Although these categories are well established, several studies have indicated the existence of more compositional groups (Picon and Vichy, 2003; Foster and Jackson, 2010).

## 2.5. Architectonic glass

The glass can be part of the decoration of the buildings in many forms. It was used for inlays for household furnishings, sacred shrines, wooden coffins and ceremonial weapons, mosaics in pavements and in walls, *opus sectile* panelling, revetment plaques and windows. The majority of these objects were produced by casting in open or closed moulds and then finished by cutting, grinding and probably polishing (Grose, 1989). Although a variety of stones usually served these functions, glass was preferred in many cases, because of its colour, its light weight and its luminosity (Grose, 1989). It was also a luxury product, so it is rarely found and exclusively in public and elite contexts (Boschetti, 2011). During the Roman period, glass industry attested a huge increase in glass production, which also included increased use of glass for architecture (Grose, 1989).

The first use of glass for decoration was attested with the glass inlays of coloured opaque glass in Egypt dating to the 14th century BC (Grose, 1989, Slough, 2005; Henderson, 2013). They were used to decorate mainly wooden sarcophagi but also household furniture. Egyptian inlays continued to be manufactured until the Ptolemaic and the Roman period, representing a distinct tradition (Henderson, 2013). They could take the form of facial features, like eyes and eyeliners, anthropomorphic or zoomorphic figures, mosaic canes and hieroglyphic signs.

Moreover, glass inlays started early to be produced in Mesopotamia. Particularly, they are found in Tchoga Zanbil, in Iran dating to the late 13th century BC, where a large number of glass inlay rods decorating the wooden doors of temples and palaces was excavated (Barag, 1985). The Phoenicians further developed the production of colourless glass inlays during the 9th-8th century BC, as it is attested in Nimrud in Assyria (Mallowan, 1947).

Between the 8th and the 4th century BC, archaeological evidence is scarce. Some findings in Olympia, Greece, in the 5th century BC suggest that glass inlays were used occasionally to embellish sculptures and buildings (Henderson, 2013). A stronger presence of glass inlays in Greece is attested in the 4th century, as they were found in sixty burials of all types in Macedonia (Ignatiadou, 2002). They usually decorated the visible front legs of the symposium couches or more rarely chests and sarcophagi. The decoration consisted of individual elements such as eyes, anthems or representations in relief. A few glass inlays are also found outside Macedonia, namely in Scythia, Tarentum and Kerameikos, which are usually attributed to Ionia. This production diminished or ceased at the beginning of the 3rd century BC. Glass inlays are also recorded often in the Roman period (Grose, 1989).

The glass was also used for mosaics of different types in the buildings. Mosaics were already in use from the beginning of the 3rd millennium BC in Mesopotamia, in the Sumerian city of Uruk (Ruggero, 2009). The material originally used was clay embedded in a mortar forming geometrical patterns on the surfaces of the columns and the walls. Mosaics continued to be produced, using mainly river pebbles until the 4th century BC when materials like ceramic fragments and glass were employed in Pella (Greece) complementary to stone to complete the colour palette (Petsas, 1965; Boschetti, 2011).

Glass started to be used systematically in mosaics at the end of the 3rd century BC (Boschetti, 2011). Egypt is usually considered the geographical origin, as twenty mosaics in *opus vermiculatum* dating to the end of the 3rd century BC attested the first extensive use of glass (Guimier-Sorbets, 2001). *Opus vermiculatum* is a mosaic technique that uses small *tesserae* cut from canes with great precision. In the 2nd century BC, the new technique spread in the Greek islands, Israel, Cyrene and Italy (Boschetti, 2011). Particularly for Italy, *opus vermiculatum* was employed mainly in the areas of Vesuvius and in Latium from the end of the 2nd century BC onwards. The *opus vermiculatum* has two special characteristics in Italy in comparison with other locations. Firstly, the *tesserae* were cut from cakes and not canes at least until the Augustan Age. Moreover, the palette of colours was quite limited in Italy, as only opaque red, blue, green, yellow and rarely orange were used (Boschetti, 2011).

Glass was usually used in *opus vermiculatum*, though some examples in *opus sectile* are also attested in Rome, in a mosaic from a house under the temple of Venus, dating at the middle 1st century BC (Morricone, 1987). *Opus sectile* is a technique in which the pattern consists of pieces of stone, shell or glass cut in irregular shapes to fit the component parts of the design. The most important technical requirement is the ability to cut the elements, as the term “sectile” is the Latin word for cutting (Ruggero, 2009). This technique was the most praised by the Romans and the most popular choice for Imperial public buildings and private elite houses (Boschetti, 2011). *Opus sectile* appeared for the first time in Italy as pavement in Republican times and as wall and ceiling decoration from the first half of the 1st century BC. From the 1st century AD, it was regularly employed for the decoration of pavements and walls (Boschetti, 2011). Glass remained a marginal material in the pavement *opus sectile*, but it was the most used material for wall decoration (Boschetti, 2011). It is worth mentioning that mosaics could be surrounded by twisted rods to make a frame. They were extensively used during the early Julio-Claudian period. The twisted rods used for architectural decoration are tightly twisted with smooth edges (Grose, 1989; Cosyns et al., 2006).



### 3. Lamia's Gardens

The Roman Gardens, more known as Roman Horti, were very popular among the Roman nobility from the Late Republican era until at least the 3rd century AD. The term *hortus* was already in use from the time of the foundation of Rome according to Varro (Varro, *De Re Rustica*). He associated it with the earth division made by Romulus. Pliny (Pliny, *Naturalis Historia XXXVI*) gives a different interpretation of the term, suggesting that it meant the plot of land assigned to the colonists in the first phase of Roman colonization. It is important to highlight that there was a change in the meaning of the word, as already in the time of Pliny it had lost its original rural character. From the Late Republic onwards, the word *horti* was related to vast green zones that often, but not necessarily, included some habitations or other structures and were built in various periods and phases (Guidobaldi, 2009). This phenomenon was encouraged especially in the part beyond the Servian walls by the abundance of water, provided by the four -later five- aqueducts located in the region.

More than sixty names of Gardens are found in ancient references, but the exact location of most of them is not precisely known (Figure 3.1). Names and zones of the majority of the Gardens are known, but further information, like their size, exact location, and the constructions that they included, is rarely available. The ones that are better recorded are located on the Esquiline and Quirinal Hills. These hills hosted the richest Gardens, and they underwent urban intervention at the end of the 19th century, which helped the recording of the archaeological remains. The most studied Gardens are those of Maecenas and of Lamia on the Esquiline Hill.



Figure 3.1 The Gardens of Rome in green, the area of Lamia's Gardens in the red circle (Cima and Talamo, 2008)

Such luxurious residential complexes outside the walls of the city were built following the examples of the architecture of the Hellenistic tradition (Barrano et al., 2007; Cursi, 2019; Barbera et al, 2010). They consisted of buildings for habitation and entertainment, such as pavilions destined to host symposia. They were also equipped with porticoes, theatres, gymnasia and temples. Moreover, they had lavish decorations with many expensive materials such as marble, alabaster and glass and many sculptures. The main aim of their owners was to express their aesthetic and cultural idea and to exhibit their wealth.

The first *hortus* mentioned was the Horti of P. Cornelius Scipius Africanus. Cicero (Cicero, *De Natura deorum* 2, 4, 11) described it in relation to a ceremony that took place there in 163 BC. A possible location might be on the slope of the Quirinal Hill (Cursi, 2019). Later, some historical sources reported of Horti belonging to Pompey and Caesar, but the real increase in the number of Horti occurred in the mid-1st century BC, when Maecenas established his own Horti on the Esquiline Hill.

The Esquiline hill, outside of the city walls, had been almost exclusively used for burials from the end of the 9th century BC until that moment (Albertoni, 1983). According to Coarelli (1993), public burials were found in the north side of the street Labicana, whereas burials of the poor in the south of this street. The burials of famous people, such as Maecenas and the poet Horace (Alagia, 2014), continued to the Late Republic along the street Labicana. Nevertheless, the aspect and intended function of the area changed radically by Gaius Maecenas (68–8 BC), Augustus's friend and advisor. He reclaimed this part of the hill to create a park. This area was assigned to him by the civil authority. It has been suggested that the exploitation of this part of the city was a plan of urban transformation promoted by Augustus himself (Cima and La Rocca, 1986; 1998). Soon after him, other luxurious habitations started to be built in the suburbs of Rome by the members of the higher classes of the Roman society.

Shortly after the establishment of the Horti, some owners started to donate their Gardens to the emperor. First, Sallustius Priscus bequeathed his Garden to Tiberius in 21 AD, and it became part of the imperial state property. Accordingly, other noblemen gave away their properties to the emperor, willingly or by force, so that at the time of Claudius most of the Gardens on the Esquiline Hill were imperial property (Cursi, 2019). Particularly, the Horti of Maecenas were the initial nucleus of an imperial park, which in the period of Nero consisted of the Esquiline, Quirinal, Pincian and Oppian Hills. Likewise, this will to control the area was connected with the proximity to the five aqueducts of Rome in this region (Paolucci, 2007).

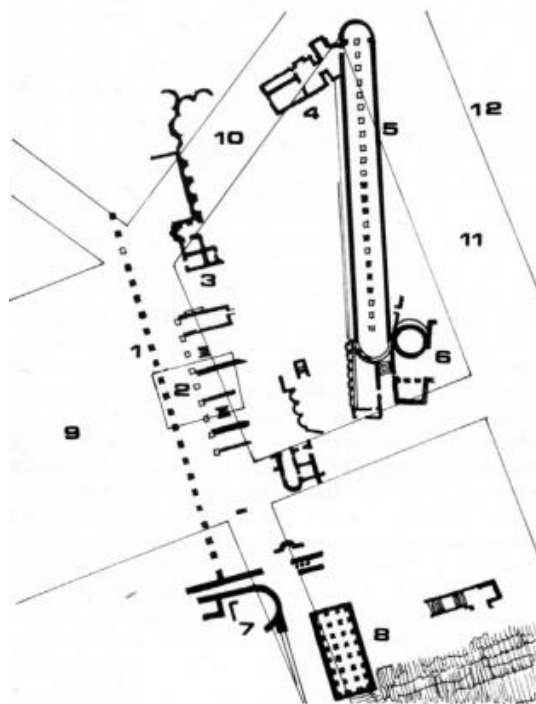
Probably the emperor's property remained substantially unified throughout the 1st century, but already in the 2nd century, probably starting under Trajan (98-117 AD), there was a series of dispersions dictated by necessity.

The complete abandonment of the Horti began in 410 AD when the Goths of Alaric burned numerous buildings and a large part of the palace (Cursi, 2019). From this period onwards, there is a preference of living inside the city walls, so that the suburban areas are abandoned. A proof for this is the existence of four burials in the Esquiline dated between the 8th and 10th century AD. As the region was not inhabited in Medieval times, it took its initial funerary function.

One of the most known and researched Horti is Lamia's Gardens. Most of the researchers agree that it was established at the end of the 1st century BC by L. Aelius Lamia, member of a rich equestrian family from Formia, consul in the year 3 AD and intimate friend of Tiberius. However, Alagia (2014) believes that it was founded before, shortly after the establishment of the Horti of Maecenas, by another member of the Lamia family. He supports that L. Aelius Lamia, the latter's father, *legatus pro praetore* of Hispania Tarraconensis in 24 BC, was the real founder. He even claims, based on Cicero (Cicero, Letters to Atticus, 12, 21, 22, 29), that the family, particularly L. Aelius Lamia, praetor in 42 BC, possessed land in the Esquiline Hill as early as the mid-1st century BC.

Lamia's Gardens bordered with the Horti of Maecenas and those of Maia with certainty and probably with the Horti of Tauria. Its exact size is not known, but most scholars adopt the indications given by Nibby and de Romanis (Nibby, 1838). In the west, the border with the Horti of Maecenas was almost with certainty the ancient street Merulana, which today coincides with the alley of San Matteo. In the east, it probably reached the current street Emanuele Filiberto. However, there is a big uncertainty on northern and southern limits. It is likely that in the north it reached the ancient street Labicana including the modern square Vittorio Emanuele, while in the south the road at the bottom of the valley traced today by the current streets Labicana and Manzoni. Certainly, the Gardens must have had considerable size, as they had their own administrator even when it was part of the united imperial property (Paolucci, 2007).

During the centuries, the Gardens underwent many construction phases to respond to the needs of its owners and trends of the period. At least 7 phases of construction activity between the last decades of the 1st century BC until the mid-3rd century AD have been mentioned (Barbera et al., 2010; Lazzara, 2019). The complex did not have a construction unity. On the contrary, it consisted of various constructions placed on natural slopes or artificial terraces with different orientation (Figure 3.2).



1. Colonnaded portico; 2. Villa Palombara; 3. Place of discovery of the Discobolus Lancellotti; 4. Underground rooms with many hidden sculptures; 5. Cryptoporticus with floor in opus sectile; 6. Thermal complex with marble floors discovered in 1875; 7. Thermal complex; 8. Cistern; 9. Piazza Dante; 10. Foscolo street; 11. Emanuele Filiberto Street; 12. Area of Villa Altieri

Figure 3.2 Lamia's Gardens: Plan of the 1873-1876 findings, between Foscolo street, Emanuele Filiberto Street and Dante Square (Lanciani, 1986)

Even before the organization of the space by Lamia, the entire area was used as a garden, as evidenced by the presence of a dense series of pole holes identified on the eastern side close to the wall, probably related to the cultivation of flowers. In this phase, real buildings seem to be missing (Barbera et al., 2010).

At the end of the 1st century BC, a building complex was erected, destroying the previous structures, which coincides with the phase of the foundation of the Gardens, soon after the reclaim works conducted by Maecenas. Among the elements of the complex, a long corridor was identified, with a length of around 9 m and a width of 2.4 m (Barrano et al., 2007). It is not possible to reconstruct with certainty if it connected different sectors of a unique pavilion or if it had the function of connecting different parts. Shortly after the phase of the foundation, an extension was arranged, that foresaw a series of rooms in the sides of the already existing corridor.

In 33 AD, under Tiberius (14-37 AD), the Gardens became part of the imperial state property. In the Julio-Claudian period, a substantial reconstruction plan of the complex occurred, as the previous articulation was only partially maintained. This vast renovation is usually associated with Caligula (37-41 AD). Ancient sources mention that Caligula had a particular preference for these Gardens, as he is pictured by Philo (Philo, *Legatio ad Gaium*) personally giving instructions for the renovation. Philo further describes a building complex composed of different architectural nuclei, alternating with green spaces, and connected by arcades, cryptoporticus, staircases and ramps.

Moreover, Suetonius (Suetonius, Caligula) records that Caligula was even temporarily buried in Lamia's Gardens until his sisters transferred his body to the royal tomb.

At the time of Caligula, the principal features of the Gardens were a large circular mausoleum along a road at the north edge of the property and three widely spaced, elongated constructions, which seem to have marked terraces on the hillside facing the ancient street Merulana. The middle construction was a portico, with pillars in front of a row of chambers. The other two elongated structures were *cryptoporticus*, *i.e.*, largely underground corridors illuminated by openings in their vaults.

In the second half of the 1st century AD, following a destruction event from which significant traces have been found, two rooms placed to the west of the corridor were repaved with mosaics. It is also assumed that these Gardens were annexed, for a short time, to Nero's Domus Aurea (Paolucci, 2007). In fact, Nero (54-68 AD) combined its properties on the Palatine with those of the Esquiline, creating a huge residence organized as a suburban villa in the centre of Rome (Suetonius, Nero; Tacitus, Annales 15).

During the 2nd century AD, the rooms of the east sector had new interventions of modernization, limited mostly to decorative elements and coating. Moreover, at this time some parts of the Gardens were sold to individuals as it is attested by the existence of two private *domus*. However, the residential area of the Gardens was still owned by the emperor (Barrano and Martines, 2006; Guspini, 2007; Alagia, 2014).

Between the end of the 2nd and the early 3rd century AD, the complex had another reconstruction of the spaces involving substantial structural interventions, probably due to problems of static nature. The corridor was enlarged demolishing the oriental limit and constructing a more eastern new wall that cut the geometric mosaic of the previous phase.

More attention was paid to the Gardens by Alessandro Severus (222-235 AD). Under his reign, the Gardens became part of the private property of the emperor as it is attested in an inscription on a fistula aquarium. Because of this fistula with the name of the emperor Alessandro Severus, Lanciani (Lanciani, 1893) believed that the residential complex was under extensive restoration in the 3rd century AD. Particularly, under his reign, the great nymphaeum and the castellum aquae, known as Mario's trophies, were built.

During the late antiquity, a series of interventions can be attested by archaeological findings, which were presented extremely incomplete and inhomogeneous. The re-use of materials is prominent, so that a systematic interpretation is not possible (Barrano et al., 2007). In the 4th century AD, the Gardens seem to be gradually abandoned, as there is no further information

about it in literary sources. Initially, the Christian communities of S. Eusebio and S. Bibiana settled on the hill. Nevertheless, the complete abandonment of the Gardens happened under Diocletian (284-305 AD), when most of the sculptures were destroyed and the materials reused for the construction of a thermal complex nearby (Bertoletti et al., 2007).

Later, the area was used again for funerary purposes as it is attested by the four graves found dating between the 8th and 10th century AD. This is the only evidence of frequentation of the site for a long time (Barbera et al, 2010).

The area attracted again some attention in the 16th century, when Pope Gregorio XIII first, and then Pope Sisto V, decided to level the zone for the construction of roads that would reach the Basilica of Saint Mary Major, the Basilica of Saint-John in Lateran and the Basilica of the Holy Cross in Jerusalem (Barrano et al., 2007). During this construction works, many ancient sculptures were found, that initially decorated the Gardens, and they are exhibited today in various museums in Europe. Their provenance from Lamia's Gardens has been reconstructed by Häuber (Häuber, 1986). For example, a complex representing the cycle of Niobites and consisting of 14 statues was discovered. This random finding of sculptures continued for the next two centuries.

In 1826 Nibby and de Romanis (Nibby, 1838) were the first to locate the position of the Gardens in the site occupied at that time by the villa Palombara and the villa Altieri. Nevertheless, the first excavations were undertaken many years after, at the end of the 19th century (Figure 3.3). They were initiated by the urbanization plan of the region in the 1870s and 1880s. Although the excavations were supervised by the Communal Archaeological Commission, they weren't thoroughly described and recorded. However, the work of Lanciani (Lanciani, 1893) provides useful information for the topography of the area and even about the material that was destroyed during the construction works. The excavations brought to light some structures, like a cryptoporticus and a long portico, inside which several rooms decorated with frescos existed. Both structures were dated to the 1st century AD. A further building nucleus found during the excavations consists of a hemicycle, which seems to be connected to a water pipeline with various cisterns, possibly a *nymphaeum* (Barbera et al., 2010). Moreover, a significant number of sculptures has been found. The most mentioned example is the discovery of a room in the north of the *cryptoporticus*, where several sculptures were found, like a sculpture of Venus Esquiline, two Muses, a torso of Dionysus, and the portrait of Commodus in the disguise of Hercules. This room has been often interpreted as a storage room, where sculptures were hidden in a period of imminent danger and never recovered (Lanciani, 1888; Cima and La Rocca, 1986; 1998; Barbera et al., 2010).

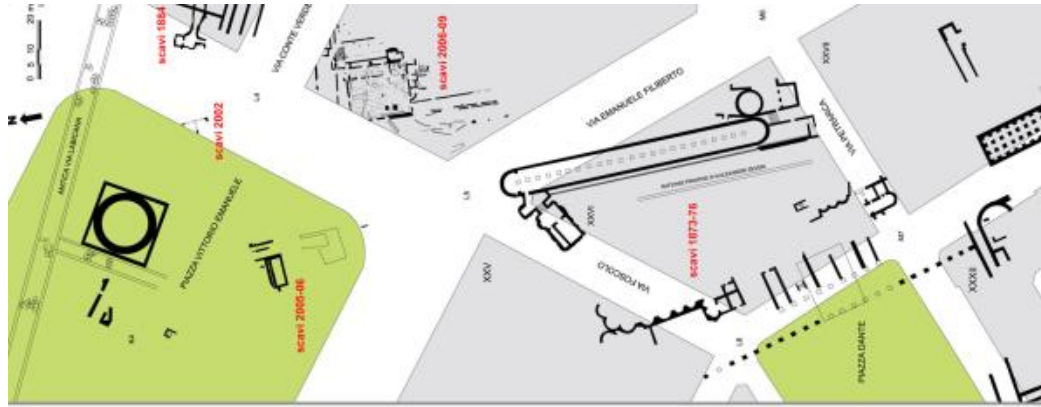


Figure 3.3 Lamia's Gardens: Topographical plan with indication of the main excavations from 1873 to 2009 (Barbera et al., 2010)

More recently, between 2002 and 2005, three geophysical surveys were carried out to know the stratigraphy and the geological characteristics of the area. The execution of core sampling confirmed the hypothesis of Lanciani about the topography of the area (Menghi, 2002; 2004; 2005).

Lastly, the construction works for the creation of the headquarters of the National Insurance and Assistance Body for Doctors and Dentists (Ente Nazionale di Previdenza ed Assistenza dei Medici e degli Odontoiatri ENPAM) initiated a rescue excavation of Lamia's Gardens. The archaeological excavation was carried out between 2006 and 2009 in the area between square Vittorio Emanuele II, street Conte Verde and street Emanuele Filiberto in Rome. It covered a total area of 1600 m<sup>2</sup> and it yielded more than eight thousand boxes of recovered artefacts. From this survey, it was possible to reconstruct and understand the architectural layout of the complex (Barrano et al., 2007; Barbera et al., 2010; Barbera, 2013).

In conclusion, the residential complex has to be imagined as an organism consisting of several parts, often differently oriented and in some cases without any topographical connection, probably due to the morphology of the area on which they stood, immersed in large gardens and connected to buildings.



## 4. Materials and methods

### 4.1. Materials

For this study the glass samples used were selected from the stratum US 2541 unearthed between 2006 and 2009 in an excavation across Lamia's Gardens. This excavation was realized due to the construction works for the new building of the National Insurance and Assistance Body for Doctors and Dentists (Ente Nazionale di Previdenza ed Assistenza dei Medici e degli Odontoiatri, shortly ENPAM) in the area between square Vittorio Emanuele II, street Emanuele Filiberto and street Conte Verde (41.893384,12.505626), which only corresponds to a part of the original Gardens. The material came from the destruction of the building they belonged to and their subsequent use as part of the foundations for the construction of the new building.

The stratum US 2541 is dated to the second half of the 2nd century AD, which is a *terminus ante quem* for the dating of the findings. Therefore, the glass fragments are dated to the second half of the 1st century AD or the first half of the 2nd century AD. Except glass, the stratum also contains fragments of marble. Among the findings from the excavation, this stratum stands out for the number and variety of glass fragments retrieved: polychrome rods with twisted section, fragments of cameo glass panels, decorative elements in the form of leaves, monochrome and polychrome fragments related to *opus sectile*, window panels, fragments with different shaped elements probably relating to furniture decoration and some vessels for a total of 6828 glass fragments.

A selection of 20 fragments of architectonic glass, representative of different colours, functions and methods of productions, were chosen to conduct an archaeometric analysis. The basic characteristics of the samples -namely colour, function and method of production- are summarized in Tables 4.1 to 4.4.



Table 4.1 Summary of the basic characteristics of the glass samples






Sample N°.	Sample	Object	Colour	Technique	Date
1		<i>Opus sectile</i> element	Opaque red	Casting	1st-2nd century AD
2		<i>Opus sectile</i> element	Opaque orange	Casting	1st-2nd century AD
3		<i>Opus sectile</i> element	Opaque red	Casting	1st-2nd century AD
4		<i>Opus sectile</i> element	Opaque yellow	Casting	1st-2nd century AD
5		Twisted rod	Opaque yellow	Handmade	1st-2nd century AD

Table 4.2 Continued from previous page






Sample N°.	Sample	Object	Colour	Technique	Date
6		<i>Opus sectile</i> element	Opaque light green	Casting	1st-2nd century AD
7		<i>Opus sectile</i> element	Opaque light green	Casting	1st-2nd century AD
8		Glassmaking waste: raw glass	Opaque white	Raw glass	1st-2nd century AD
9		<i>Opus sectile</i> element	Opaque white	Casting	1st-2nd century AD
10		Twisted rod	Opaque white	Handmade	1st-2nd century AD

Table 4.3 Continued from previous page

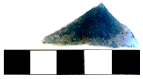









Sample N°.	Sample	Object	Colour	Technique	Date
11		<i>Opus sectile</i> element	Opaque light blue	Casting	1st-2nd century AD
12		<i>Opus sectile</i> element	Opaque blue	Casting	1st-2nd century AD
13		Twisted rod	Transparent blue	Handmade	1st-2nd century AD
14		Plaque	Cameo glass	Casting	Late 1st c. BC- Early 1st c. AD
15		Plaque	Cameo glass	Casting	Late 1st c. BC- Early 1st c. AD

Table 4.4 Continued from previous page

Sample N°.	Sample	Object	Colour	Technique	Date
16		Plaque or vessel fragment	Opaque red, yellow, white, brown, black (mosaic glass)	Casting (mosaic)	1st century AD
17		Glassmaking waste: section of cane for mosaic glass plaque or vessel	Opaque red, yellow, white, brown, black	Handmade	1st century AD
18		Glassmaking waste: cane for mosaic glass plaque or vessel	Opaque red, yellow, white, brown, black	Handmade	1st century AD
19		Plaque in the shape of a leaf	Opaque green, light blue, yellow, black	Casting (mosaic)	1st century AD
20		Glassmaking waste: cane for mosaic glass	Opaque yellow, black	Handmade	1st century AD

## 4.2. Methods

### 4.2.1. Sample preparation

For the preparation of the samples, micro-sampling was performed by dry-cutting small fragments, which were then embedded in the HARDROCK 554 epoxy resin to obtain polished cross-sections (Figure 4.1). After Optical Microscopy examination, samples were carbon coated to be analysed by Scanning Electron Microscopy coupled with Energy Dispersive Spectroscopy (SEM-EDS), followed by Electron Microprobe Analysis (EMPA) and Laser Ablation Inductively Coupled Plasma Mass Spectrometry (LA-ICP-MS).



Figure 4.1 Seven pill moulds with the mounted samples

### 4.2.2. Analytical Methods

#### 4.2.2.1. Optical Microscopy

To study sample morphology and specifically, the existence of bubbles, inclusions and alterations in the glass, Optical Microscopy on the cross-sections was performed using a SZ-CTV OLYMPUS light microscope.

#### 4.2.2.2. Scanning Electron Microscopy-Energy Dispersive X-Ray Spectroscopy (SEM-EDS)

For sample morphology and major chemical composition analysis by SEM-EDS, a FEI Quanta 400 Scanning Electron Microscope (Figure 4.2) operating with accelerating voltage of 20 kV and high vacuum of 130 Pa was used coupled to an EDS detector. Elemental data were obtained by point microanalyses.



Figure 4.2 Scanning Electron Microscope FEI-QUANTA 400 (SEM-EDAX)

#### 4.2.2.3. Electron Microprobe Analysis (EMPA)

Electron Microprobe Analysis (EMPA) was performed by a CAMECA SX50 Electron Microprobe (Figure 4.3) equipped with five wavelength-dispersive spectrometers operating at an accelerating voltage of 15 kV and a beam current of 15.1 nA. Four-to-five-point analyses were conducted for each sample. More points were chosen when the sample consisted of different colours. The first four samples (Table 4.1) were analysed in manual mode, and the rest in automatic mode. Matrix corrections were calculated by the software supplied by Microbeams Services with the PAP procedure (Pichou and Pouchoir, 1985). The detection limits were in a range between 0.01 and 0.1 wt% under the specified conditions. The references for quantitative analysis are mentioned in Table 4.5.



Figure 4.3 Electron microprobe CAMECA SX50

Table 4.5 References used for the quantitative analysis of the chemical elements

References	Elements
Wollastonite	Si (on the TAP, thallium acid phthalate crystal), Ca (on the PET, pentaerythritol crystal)
Periclase	Mg (on the TAP)
Corundum	Al (on the TAP)
Jadeite	Na (on the TAP)
Magnetite	Fe (on the LIF, lithium fluoride crystal)
Orthoclase	K (on the PET)
Apatite	P (on the PET)
Barite	S (on the PET)
Rutile	Ti (on the PET)
Galena	Pb (on the PET)
Cassiterite	Sn (on the PET)
Chalcopyrite	Cu (on the LIF)
Phlogopite	F (on the LIF)
InSb	Sb (on the PET)
KCl	Cl (on the PET)

#### 4.2.2.4. Laser Ablation Inductively Coupled Plasma Mass Spectrometry (LA-ICP-MS)

LA-ICP-MS analysis was performed at HERCULES Laboratory at the University of Évora, Portugal, using a CETAC LSX-213 G2+ Laser Ablation system coupled to an Agilent 8800 Triple Quad Mass Spectrometer.

Samples were measured together with the certified reference glass NIST 610 for method validation and external calibration. NIST 612 and GSE-1G reference materials were also analysed as blind samples for quality control (QC) assays.

The laser ablation system operated in spot-analysis mode, set up with 100 µm spot diameter, 400 burst count, with 100 % of output energy using a repetition rate of 20 Hz and a total acquisition time of 50 s (10 s of gas blank, 20 s of sample ablation and 10 s of washout). Summary and further information of operating conditions are presented in Table 4.6 and Table 4.7. Additionally, the dwell times of the isotopes analyzed are displayed in Table 4.8

Table 4.6 Operating conditions of the laser

<b>Laser type</b>	<b>Q-switched Nd: YAG laser</b>
Wavelength (nm)	213
Laser Ablation Chamber	CETAC LSX
Ablation Mode	Single-spot (400 shots)
Spot size (µm)	100
Output energy	100%
Repetition rate (Hz)	20
He carrier gas flow rate (L min <sup>-1</sup> )	1

Table 4.7 Operating conditions of the ICP-MS system

<b>ICP-MS</b>	<b>AGILENT™ 8800 Triple Quad</b>
Mode	SQ (Single Quad)
RF Power (W)	1200
Acquisition time (s)	20 s of ablation, 10 s gas blank, 10 s washout
Ar Plasma gas flow rate (L min <sup>-1</sup> )	15
Ar Auxiliary gas flow rate (L min <sup>-1</sup> )	1

Table 4.8 Isotopes analyzed by LA-ICP-MS and their dwell times

<b>Dwell time (ms)</b>	<b>Isotope</b>
2	<sup>28</sup> S
5	<sup>47</sup> Ti, <sup>5</sup> Mn, <sup>66</sup> Zn
10	<sup>59</sup> Co, <sup>63</sup> Cu, <sup>118</sup> Sn, <sup>121</sup> Sb
20	<sup>45</sup> Sc, <sup>51</sup> V, <sup>52</sup> Cr, <sup>60</sup> Ni, <sup>85</sup> Rb, <sup>88</sup> Sr, <sup>89</sup> Y, <sup>90</sup> Zr, <sup>93</sup> Nb, <sup>107</sup> Ag, <sup>111</sup> Cd, <sup>133</sup> Cs, <sup>137</sup> Ba, <sup>139</sup> La, <sup>140</sup> Ce, <sup>141</sup> Pr, <sup>146</sup> Nd, <sup>147</sup> Sm, <sup>153</sup> Eu, <sup>157</sup> Gd, <sup>159</sup> Tb, <sup>163</sup> Dy, <sup>165</sup> Ho, <sup>166</sup> Er, <sup>169</sup> Tm, <sup>172</sup> Yb, <sup>175</sup> Lu, <sup>178</sup> Hf, <sup>181</sup> Ta, <sup>197</sup> Au, <sup>108</sup> Pb, <sup>109</sup> Bi, <sup>232</sup> Th, <sup>238</sup> U



## 5. Results

### 5.1. Macroscopic and microscopic analysis

Most of the samples are heterogeneous, as they include many bubbles of different size and inclusions of different colours. Samples No.1 (Figure 5.1), No.2 (Figure 5.2), No.3 (Figure 5.3), No.7 (Figure 5.7) and No.15 (Figure 5.15) are quite homogeneous without visible inclusions or big bubbles. Many samples have inclusions of different colour (Figure 5.6; Figure 5.19). Most of the samples show signs of degradation, such as loss of colour (Figure 5.3) and iridescence (Figure 5.13).

Sample No.1 shows some white and dark spots on the surface even to the naked eye. Its surface is smooth. Loss of colour is observed around the edges. The back side is totally white with some small round gaps and some darker spots. The surface is rough. Through its observation by optical microscopy, it was found homogeneous with no inclusions and only a few circular bubbles. It presents some deterioration on the edges, as it has a few fractures (Figure 5.1).

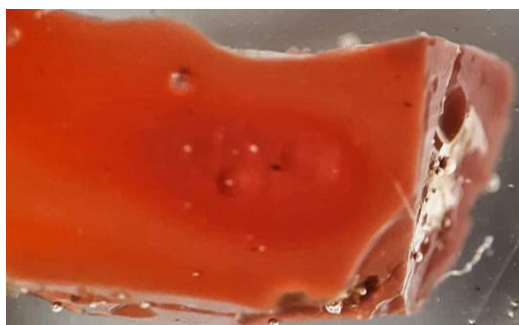


Figure 5.1 Image of sample No.1 taken by OM

The surface of sample No.2 is rough with some visible loss of colour on the edges. Some white spots and dark lines are also observed. The back side of the sample is black with some exfoliations, which reveal the orange glass. This side is smooth and homogeneous. Under optical microscope, the sample seems homogeneous with no bubbles and only two black rectangular inclusions. Its state of preservation is very good with no detectable signs of deterioration (Figure 5.2).



Figure 5.2 Image of sample No.2 taken by OM

On both sides of sample No.3, the surface is rough and heterogeneous with many visible white and grey inclusions. Optical microscopy confirmed that it is heterogeneous. Many circular bubbles of different size, cracks and inclusions could be observed. The state of preservation is not very good, as there is an extensive loss of colour in the whole sample (Figure 5.3).

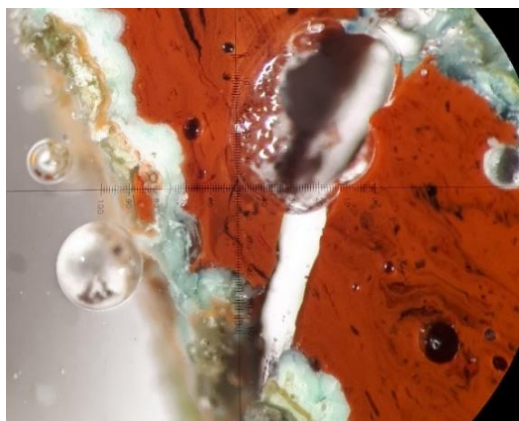


Figure 5.3 Image of sample No.3 taken by OM

On the front side of sample No.4, the surface is smooth and quite homogeneous with some black spots. Additionally, a loss of colour is observed at the outer part of the slag as it is paler. The other side is similar, but it presents less colour loss and more inclusions. With the aid of optical microscopy, one big black circular inclusion, some smaller elongated black inclusions and a few circular bubbles of different sizes were revealed. Its state of preservation is good, except some colour loss on one edge (Figure 5.4).



Figure 5.4 Image of sample No.4 taken by OM

The surface of sample No.5 is rough with some engraved lines. Two fragments were embedded, one parallel to the surface and one parallel to the diameter. The section of the surface shows that it is a quite heterogeneous glass. It has many orange and black inclusions, but not bubbles. The inclusions are both circular and elongated. Both sections have strong iridescence (Figure 5.5).



Figure 5.5 Image of sample No.5 taken by OM

The surface of sample No.6 is rough and heterogeneous. It has many small circular white and dark spots and big brownish spots. It is paler to the edges due to colour loss. On the back it is more homogeneous, as it has fewer inclusions. It has colour loss in different parts of the surface and some reddish spots at one edge. Under optical microscope, the sample is very heterogeneous with many bubbles and inclusions of black, yellow and red colour (Figure 5.6). The iridescence is evident on the outer part.

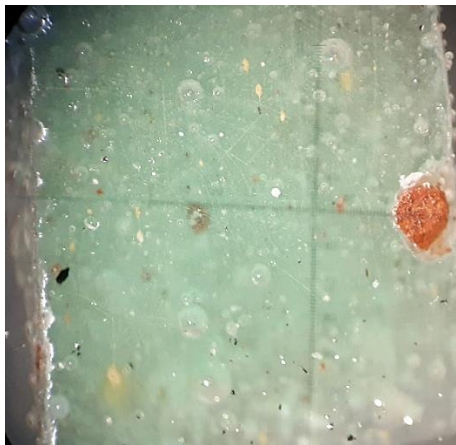


Figure 5.6 Image of sample No.6 taken by OM

Sample No.7 has a rough and heterogeneous surface. A lot of white, dark green and brownish spots are visible. The backside is more homogeneous (Figure 5.7). The sample is mostly white, but a light green area is also visible at one edge. Optical microscopy revealed a more homogeneous glass with some small circular bubbles. There are signs of degradation on the surface regarding the colour loss in some outer parts.



Figure 5.7 Image of sample No.7 taken by OM

On the front side, sample No.8 seems smooth, quite homogeneous with only some circular small black spots and some colour loss on one edge. The other side has more and bigger inclusions, but no colour loss is visible. However, under optical microscope, it seems quite heterogeneous with some elongated white and some small black circular inclusions. There is evidence of deterioration on the edges as there is iridescence and some cracks (Figure 5.8).



Figure 5.8 Image of sample No.8 taken by OM

On both sides, sample No.9 appears to be grey to the naked eye. It is smooth and homogeneous. It has some white and black circular spots of different size. Some colour loss is noticeable on the outer part. Optical microscopy showed that the glass is heterogeneous with many small circular bubbles, small black and reddish inclusions. The poor conservation state is evident by iridescence (Figure 5.9).

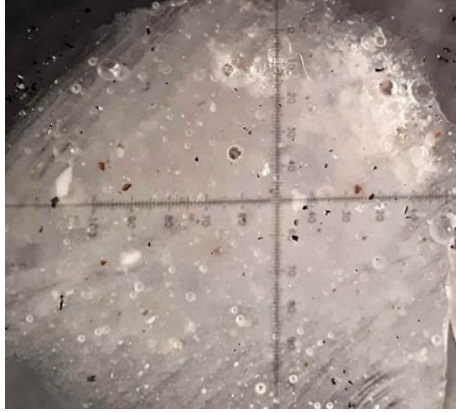


Figure 5.9 Image of sample No.9 taken by OM

Sample No.10 has a homogeneous and smooth surface with engraved lines. There are no visible inclusions. Under optical microscopy, the sample seems very homogeneous without visible bubbles, but it has a big yellow spot with two small black inclusions (Figure 5.10).



Figure 5.10 Image of sample No.10 taken by OM

The front side of sample No.11 is quite heterogeneous with small red and white inclusions. Its surface is smooth. It presents an extensive colour loss. The backside has many small white spots and a more expanded colour loss. Optical microscopy confirmed the heterogeneity of the glass, as it shows the existence of many bubbles of different size and inclusions of red, yellow and black colour. It shows signs of deterioration, as there is colour loss on the edges and iridescence (Figure 5.11).

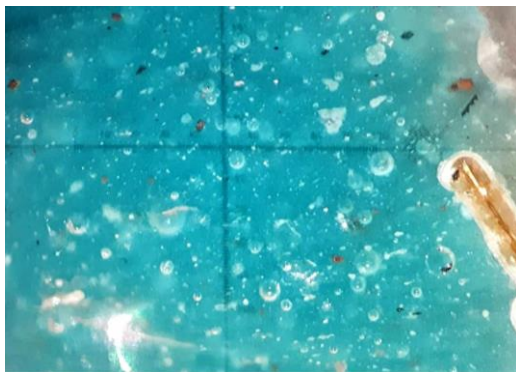


Figure 5.11 Image of sample No.11 taken by OM



Sample No.12 has a rough surface, and it seems quite heterogeneous with many white and dark spots. Colour loss is also visible. On the backside, the blue colour is covered with a grey layer. It has some black spots of different size and some white lines. Under optical microscope, the heterogeneity is more visible. Many inclusions of red, black and white colour and different size, as well as small circular bubbles, can be distinguished. It is not very well preserved as there are signs of degradation, such as colour loss and iridescence. Colour loss is evident on the edges, whereas iridescence is visible on the entire surface of the sample (Figure 5.12).

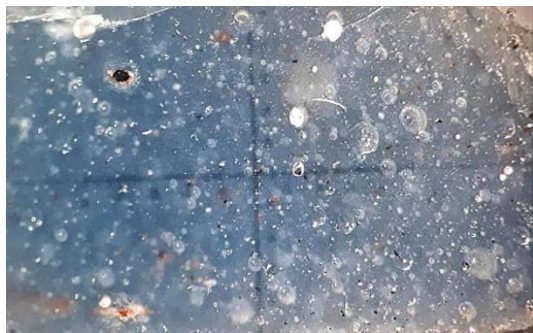


Figure 5.12 Image of sample No.12 taken by OM

Sample No.13 is decorated with painted black lines. It has different hues of blue and many white spots. The surface is smooth and homogeneous. It is shining. Under optical microscope, the glass is heterogeneous with many black, white and brown inclusions. It has a strong glow. Its state of conservation is quite good to the naked eye, but the microscope revealed an extensive degradation visible as iridescence (Figure 5.13).

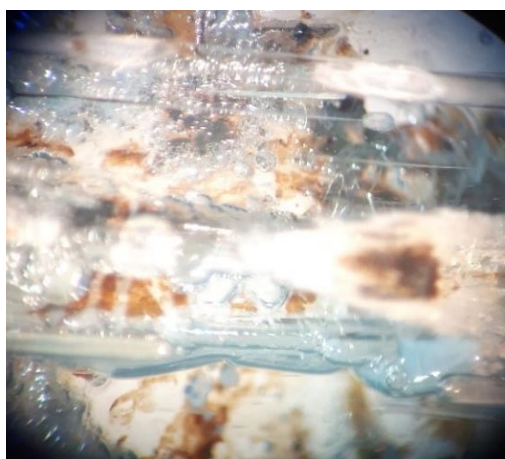


Figure 5.13 Image of sample No.13 taken by OM

Sample No.14 consists of a translucent light blue and opaque white glass. On one side, it has a heterogeneous and rough surface. It is white with many black circular and linear spots. A colour loss is evident in some parts. On the backside, it is homogeneous and smooth. It is translucent blue. A colour loss is also observed on the edges. Three thin sections of the cameo glass were

examined under optical microscope. The first section came from the white opaque surface. It shows that the white glass is very homogeneous without any bubbles or inclusions, while the blue transparent glass has many small circular bubbles and some black inclusions (Figure 5.14). The second section focuses on the blue glass. It shows that it is homogeneous with few bubbles, some dark spots and white lines. The third section comes solely from the transparent blue glass. It is very homogeneous and smooth. It has a good state of preservation.

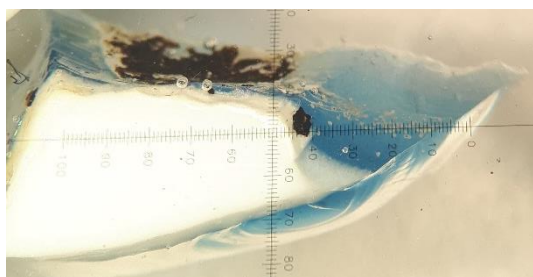


Figure 5.14 Image of sample No.14 taken by OM

Sample No.15 is translucent blue and opaque white. On the front side, it is white. Its surface is rough and heterogeneous with many black and brown spots. On the backside, it is mostly covered by a white patina. It is homogeneous and smooth. The section was taken from the white side of the cameo glass. Under optical microscopy, it showed that the white glass is very homogeneous without any inclusions or bubbles (Figure 5.15).

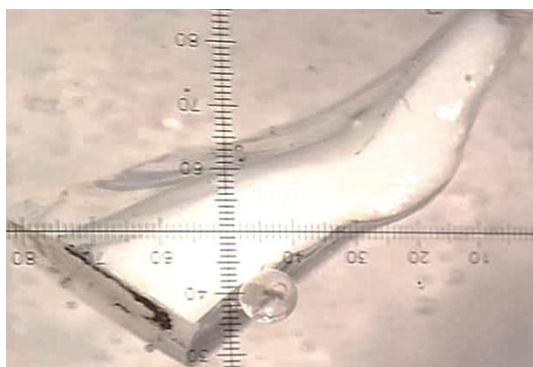


Figure 5.15 Image of sample No.15 taken by OM

On one side, the surface of sample No.16 is smooth. The mosaic glass consists of a pattern with circles of brown, red and black. The surface is a little worn. The back side is black with many white lines. It is rough and heterogeneous. Optical microscopy confirmed its heterogeneity. There are many inclusions in all the colours and some bubbles. Particularly, the white area in the centre has many white circles of different sizes and many red spots. The brown area has some white inclusions of various sizes. The red one has some lines in darker red colour, many white circles and some bubbles. Lastly, the black area is homogeneous. The deterioration is visible, as the colour peeled off in some parts (Figure 5.16).

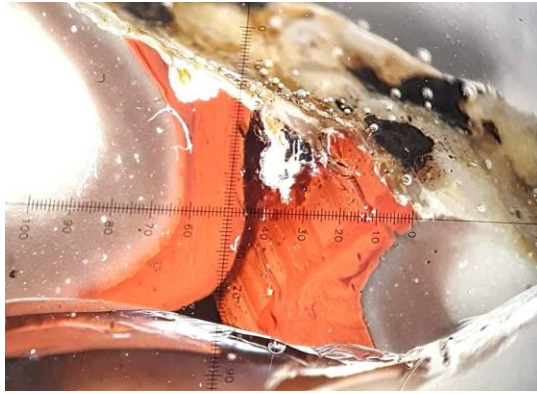


Figure 5.16 Image of sample No.16 taken by OM

Macroscopically, sample No.17 appears dark grey with a black dent in the middle. The surface is smooth and homogeneous. The outer part appears to have suffered colour loss. Optical microscopy revealed a variety of colours for this glassmaking residue. In the centre, it is white with many black spots. It is surrounded by brown glass, which has white and black spots and some light grey lines. The red glass has some black and dark spots and black lines. The outer line is black, which is the only homogeneous part of the whole sample. Degradation signs are evident due to the existence of fractures and loss of colour (Figure 5.17).



Figure 5.17 Image of sample No.17 taken by OM

Sample No.18 has a rough and heterogeneous surface. Moreover, some colour loss is visible. Under optical microscope, the variety of colour of this glassmaking waste is evident. In the centre, the glass is white with a big number of circular and elongated black spots of different size. It is surrounded by a brown circle with some white and grey small spots and some black spots of different sizes. Then, the red circle has many white spots and black lines. Lastly, the outer circle of black colour is more homogeneous, but it has some white spots. On the edges, there are evident signs of degradation, namely loss of colour (Figure 5.18).



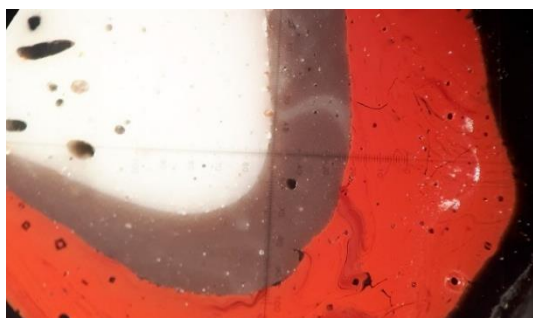


Figure 5.18 Image of sample No.18 taken by OM

The surface of sample No.19 is quite heterogeneous and rough with many white spots. In the middle there are two parallel black lines. Between them, the green hue is different than in the rest of the sample. On the other side, the glass is quite eroded. Its original colour was light green, as it can be seen in the core, which is now covered by a white patina in many parts. There are also some black spots. Optical microscopy showed that there are three different hues of green. The glass is quite heterogeneous with many inclusions in yellow, red and black colour and many bubbles (Figure 5.19). The black glass is homogeneous with a few small circular bubbles. There are degradation signs, as the colour has been lost in some parts.



Figure 5.19 Image of sample No.19 taken by OM

Sample No.20 is very fragile, as it shatters very easily. Under optical microscope, several colours were revealed in the glassmaking waste. The biggest part of the sample is yellow. The yellow glass is heterogeneous with orange, brown and dark yellow inclusions. The centre is covered by a line, black, white and red in colour, with shiny appearance. The glass does not have any bubbles. It shows iridescence (Figure 5.20).



Figure 5.20 Image of sample No.20 taken by OM

## 5.2. SEM-EDS

The results of SEM-EDS confirmed, as noted by optical microscopy, that most of the samples are heterogeneous, as they have many bubbles of different size except samples No.3, No.7 and No.13 (Figure 5.27). Many of the observed bubbles are spherical, except in sample No.10 (Figure 5.25), which has elongated bubbles. The size of these bubbles differs, but they do not exceed 200  $\mu\text{m}$  in diameter. Most of the samples have bubbles smaller than 100  $\mu\text{m}$  except samples No.3 (Figure 5.23) and No.8.

The chemical composition of the glass is homogeneous, characterized by high amounts of silicon, sodium, calcium, as they are all silica-soda-lime glasses. Diffused inclusions in the glass show high concentration of Sb and Ca except samples No.2 (Figure 5.21) and No.11, which show high concentration of Sn. Samples No.2 and No.3 (Figure 5.22) have high concentration of Cu. It is worth mentioning the high concentration of Pb in samples No.1, No.2, No.3 (Figure 5.23), No.4, No.5, No.7, No.17 and No.20.

Signs of weathering were detected in all samples. All the deteriorated parts have less sodium when compared to the bulk (Figure 5.24).

SEM-EDS revealed that sample No.1 is of the silica-soda-lime type with very high concentration of Pb and significant amount of Al and Cu. It has circular bubbles of different sizes, between 50 and 200  $\mu\text{m}$ . It has signs of extensive degradation on the edges.

Sample No.2 is a silica-soda-lime glass with elevated concentrations of Pb, Mg, Al and Cu, whereas the inclusions of the opacifier have a considerable amount of Sn and Ca (Figure 5.21). It is quite heterogeneous, as there are many signs of devitrification on the surface and some small circular bubbles. Signs of devitrification are observed in the whole surface of the glass.

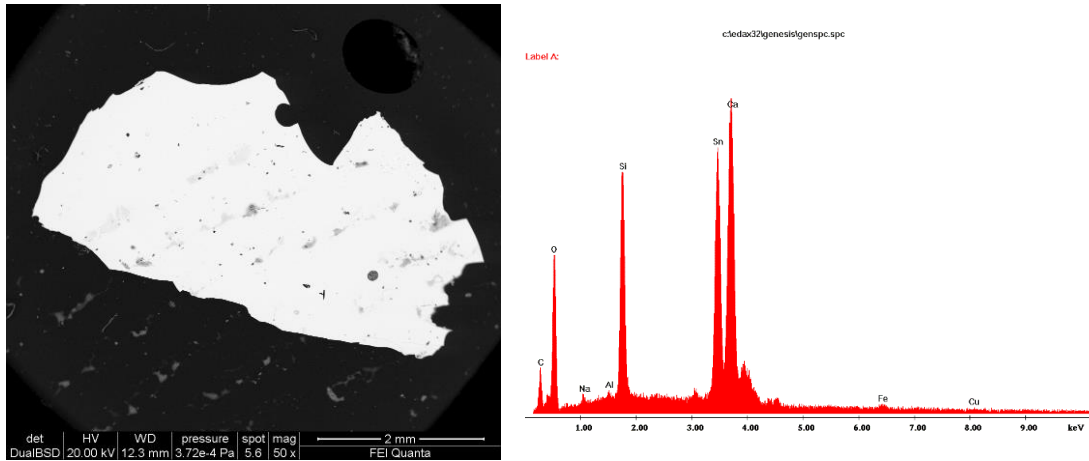


Figure 5.21 SEM image of sample No.2 and its respective bulk spectrum taken by EDS as an example of glass with a tin and calcium-rich opacifier

SEM-EDS demonstrated that sample No.3 is a typical silica-soda-lime glass with significant concentration of Pb, Mg and Al (Figure 5.22). It is quite homogeneous with some small circular bubbles (Figure 5.23) and one inclusion. Signs of degradation are visible on the edges. The chemical analysis showed that the inclusion is actually a deteriorated surface with less sodium than the bulk glass.

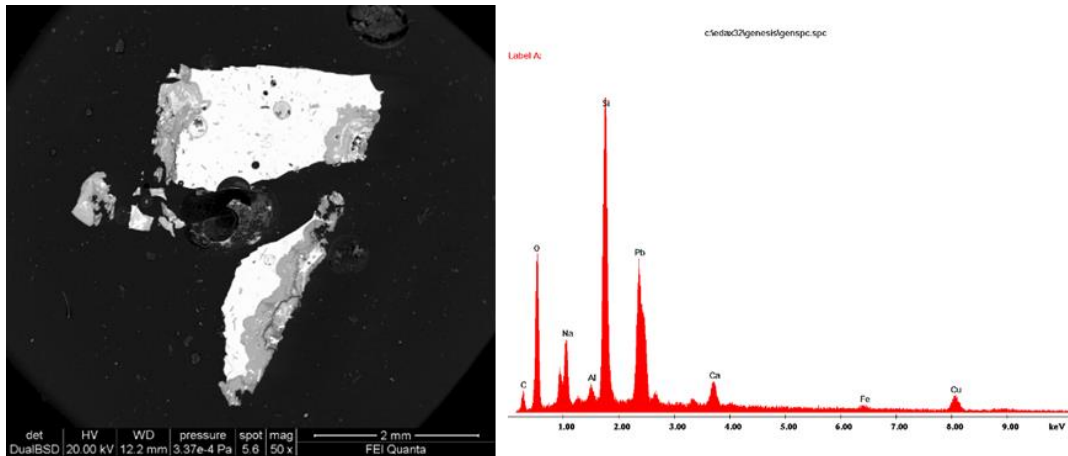


Figure 5.22 SEM image of sample No.3 and its respective bulk spectrum taken by EDS as an example of glass with high concentration of lead and copper

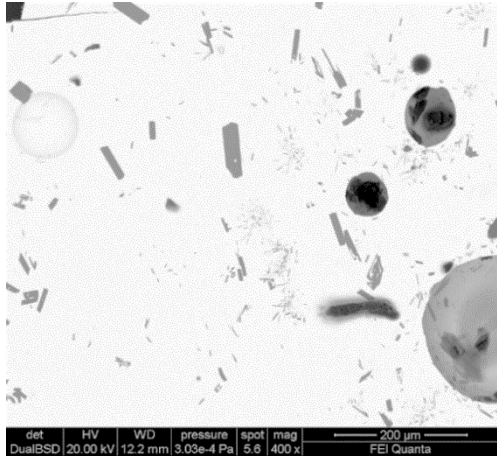


Figure 5.23 SEM image of sample No.3 as an example of big circular bubbles

Sample No.4 is a silica-soda-lime glass with considerable amount of Pb and Al. The chemical analysis of the opacifier inclusions showed increased concentration of Sb, Pb, Fe and Ca. It has some small circular bubbles which reach up to 25  $\mu\text{m}$ . There is deterioration on the edges.

The main constituents of sample No.5 are silica, soda and lime with a high level of Pb and Al. The deteriorated surface is poor in sodium (Figure 5.24). The opacifier is distinguishable by the higher concentration of Sb, Ca, Pb and Fe. It has some circular bubbles, that are smaller than 10  $\mu\text{m}$ . An extensive deterioration was also visible.

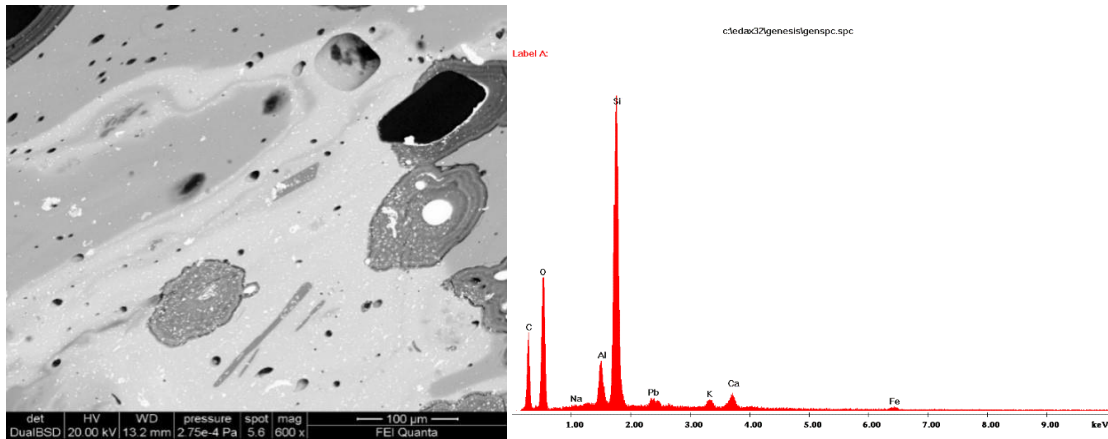


Figure 5.24 SEM image of sample No.5 and its respective bulk spectrum taken by EDS as an example of low levels of sodium

The matrix of sample No.6 consists of Si, Na and Ca with a considerable amount of Al. The opacifier is based on Sb, Ca, Pb and Fe. It has only a few bubbles of different size up to 30  $\mu\text{m}$ . The degradation is evident on two of the edges.

Sample No.7 is a silica-soda-lime type with a high level of Pb and Al. The opacifier inclusions have significant concentrations of Sb, Pb, Ca, Fe and Sn. SEM-EDS confirmed the observations made by optical microscopy. The

glass is homogeneous with a few small, circular bubbles. The degradation is visible on one side.

The chemical analysis of sample No.8 showed that the glass is of silica-soda-lime type with a considerable amount of Mg and Al, whereas the opacifier consists of Sb and Ca. It has a few circular bubbles of different size, that can reach 200  $\mu\text{m}$  in diameter. The deterioration is evident on two edges.

The glass sample No.9 consists of Si, Na and Ca with some Al and Mg. The opacifier inclusions have high levels of Sb and Ca. It has many bubbles in different size, up to 80  $\mu\text{m}$ . Some deterioration is also visible on one edge.

Sample No.10 is a silica-soda-lime glass with an opacifier based on Sb and Ca. SEM-EDS showed more details and revealed the heterogeneity of the glass, as several elongated small bubbles were visible (Figure 5.25). Additionally, an extensive deterioration on the edges was observed.

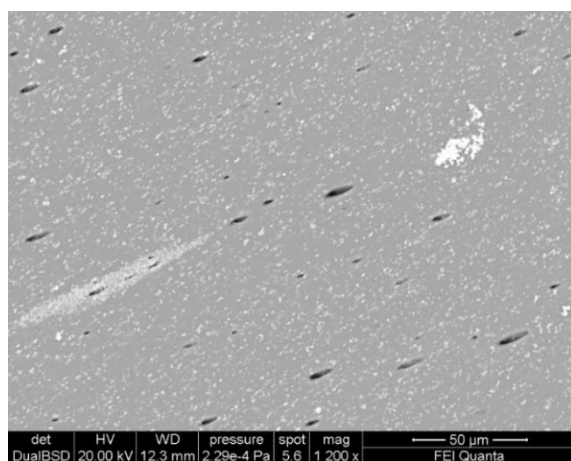


Figure 5.25 SEM image of sample No.10 as an example of elongated bubbles

The glass sample No.11 belongs to the silica-soda-lime type with a significant amount of Al and Mg. The opacifier inclusions are based on Sb, Ca and Sn. It has a few small and circular bubbles. An extensive deterioration is evident on the edges.

The glass sample No.12 consists of Si, Na and Ca with a significant amount of Al. The opacifier inclusions have higher concentration of Sb and Ca. It shows many bubbles of different size, up to 70  $\mu\text{m}$ . A black inclusion rich in Ti and Fe was also visible (Figure 5.26).



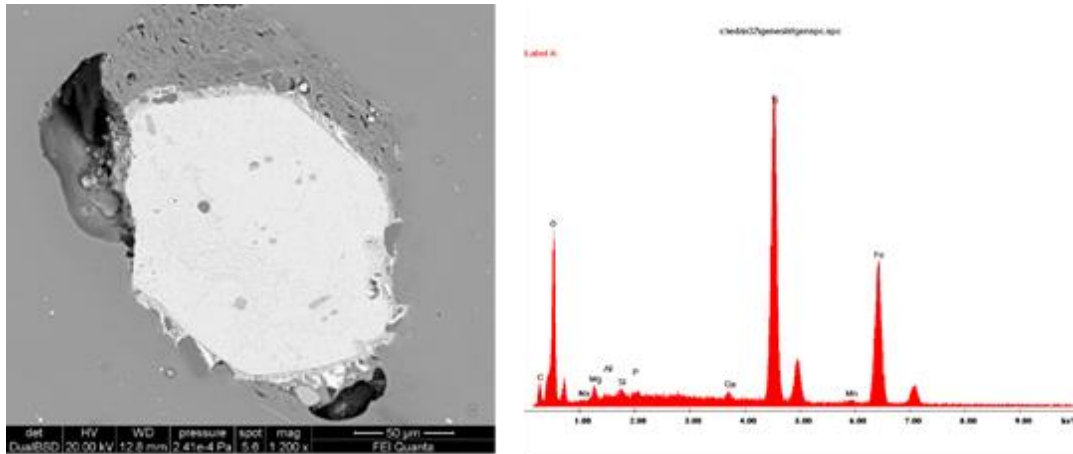


Figure 5.26 SEM image of a titanium and iron-rich inclusion from sample No.12 and its respective spectrum taken by EDS

The glass sample No.13 is a silica-soda-lime type with a distinguishable level of Al and K. It seems homogeneous under SEM-EDS, as it showed the existence of a few small circular bubbles in the glass (Figure 5.27). There is deterioration on the edges.

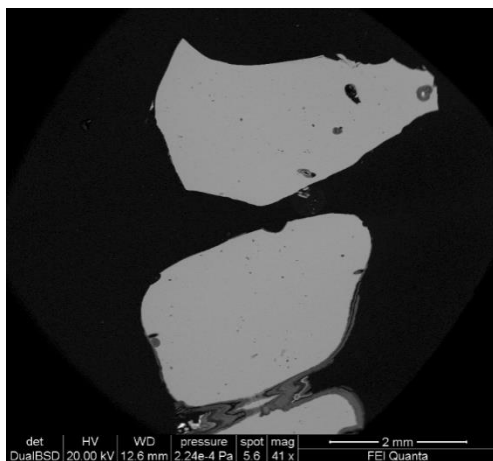


Figure 5.27 SEM image of sample No.13 as an example of homogeneous glass with a few bubbles

The main constituents of the glass sample No.14 are Si, Na and Ca with a discernible concentration of Al. The opacifier is made of Sb and Ca. For all the cross-sections, many small circular bubbles (up to 25  $\mu\text{m}$ ) were visible by SEM-EDS. The glass is quite heterogeneous. There is deterioration on the edges.

The glass sample No.15 is a silica-soda-lime type with a significant concentration of Al. The opacifier consists of Sb and Ca. It is quite heterogeneous due to the existence of a few small and circular bubbles. There are some visible fractures and some alteration on the edges.

The chemical analysis showed that all colour types of sample No.16 are made of a silica-soda-lime glass with significant concentrations of Mg and Al. The opacifier of the white and brown glass is based on Sb, Ca and Mn.

Additionally, the red glass has a considerable amount of Pb and K, whereas the black has Mn and Fe. It has a few small, circular bubbles in all the colours except the red, which is homogeneous. The deterioration is extensive, as it expands on the edges and on the interior of the glass.

The glass sample No.17 is a silica-soda-lime type with a considerable amount of Mg and Al. The white glass also has a higher concentration of Mn. The brown glass can be distinguished due to the presence of Fe and K. Its opacifier consists of Sb, Ca and Mn. The red glass has a considerable concentration of Pb and K and a low amount of Fe and Cu. Lastly, the black glass has a small amount of Mn and Fe. SEM-EDS analysis confirmed the heterogeneity. It showed an extensive deterioration on the whole surface (Figure 5.28). It has many circular bubbles of different size. Bubbles are no bigger than 50  $\mu\text{m}$ .

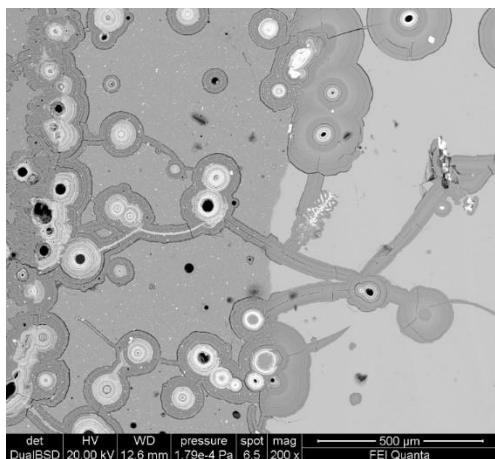


Figure 5.28 SEM image of sample No.17 as an example of extensive superficial deterioration

The chemical analysis of sample No.18 showed that it is a silica-soda-lime glass with a considerable amount of Mg and Al. The opacifier of the white and brown glass is based on Sb. The white glass distinguishes due to the presence of K and Mn in small amount. The red glass has higher concentration of Pb and K and a low concentration of Fe and Cu. Lastly, the black glass has a small amount of Mn. It presents many circular bubbles of different size, up to 80  $\mu\text{m}$ .

The main constituents of the glass sample No.19 are Si, Na and Ca with a significant amount of Mg and Al. The opacifier of all the hues of the green glass is based on Sb, Ca, Al, Pb and Fe. The inclusion found in the light green area in the middle of the sample is rich in Al, Fe and K (Figure 5.29). The black glass differs from the green because of the low amount of K and Mn. SEM-EDS analysis shows the existence of many circular, small bubbles in all the hues of green, whereas the black glass is homogeneous.

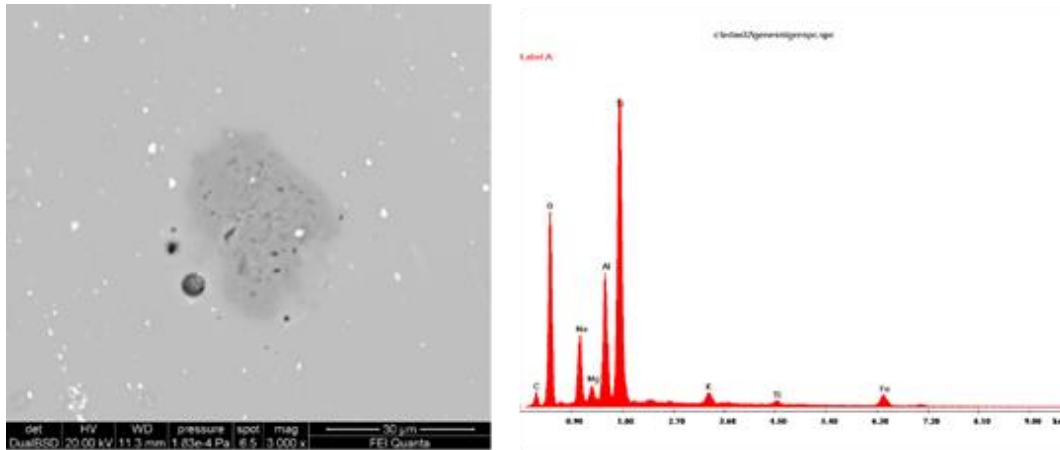


Figure 5.29 SEM image of an aluminum, iron and potassium-rich inclusion from sample No.19 and its respective spectrum taken by EDS

The glass sample No.20 is a silica-soda-lime type. The yellow glass is distinguished by the presence of Pb and Al, whereas the black glass has Al and Mn. The opacifier has higher levels of Al, Sb, Ca, Pb and Fe. It has a considerable number of cracks on the yellow glass and an extensive deterioration on the black glass. Only a few small, circular bubbles are visible.

### 5.3. EMPA

Silica concentration ranges between 39.46 and 82.52 wt%, Na<sub>2</sub>O between 0.01 and 15.54 wt% and CaO between 3.11 and 9.64 wt%. K<sub>2</sub>O varies from 0.15 to 2.21 wt%. Additives such as PbO were found between 0.01 and 40.38 wt%. Elements related to impurities of the raw materials such as Al<sub>2</sub>O<sub>3</sub>, Fe<sub>2</sub>O<sub>3</sub> and MgO are between 1.24 and 3.23 wt%, 0.3 and 2.09 wt% and 0.45 and 3.28 wt% respectively. Finally, the content of CuO is between 0.01 and 8.96 wt% and of Cl is between 0.36 and 1.11 wt%.

All major oxides plus chlorine obtained by EMPA are displayed in Table 5.1 and Table 5.2



Table 5.1 Major oxides (in wt%) measured by EMPA

Sample No.	P <sub>2</sub> O <sub>5</sub>	SiO <sub>2</sub>	TiO <sub>2</sub>	Al <sub>2</sub> O <sub>3</sub>	Sb <sub>2</sub> O <sub>3</sub>	MgO	CaO	MnO	FeO	CuO	SnO	PbO	Na <sub>2</sub> O	K <sub>2</sub> O	Cl
<b>1(red)</b>	0.04	71.75	0.07	2.52	0.64	0.54	5.36	0.05	0.53	0.06	0.01	7.76	8.69	0.53	0.98
<b>2 (orange)</b>	0.75	41.99	0.30	3.23	1.11	1.56	7.38	0.22	2.09	8.32	0.92	22.73	7.33	1.24	0.36
<b>3 (red)</b>	0.59	58.88	0.13	2.25	0.28	2.13	8.63	0.38	1.19	1.76	0.21	9.89	10.96	1.54	0.86
<b>4 (yellow)</b>	0.27	41.05	0.08	1.93	0.37	0.70	3.11	0.16	1.12	8.96	0.64	33.19	6.95	0.74	0.42
<b>5(colourless)</b>	0.09	72.71	0.04	2.73	n.d.	0.56	8.21	0.49	0.30	0.02	0.01	0.03	12.94	0.69	0.89
<b>5(yellow)</b>	0.08	61.80	0.04	2.31	1.13	0.45	7.02	0.08	1.03	0.01	0.07	16.61	7.83	0.48	0.62
<b>6(green)</b>	0.05	73.46	0.06	2.33	0.70	0.57	6.16	0.16	0.6	1.21	0.05	0.85	11.68	0.54	1.11
<b>7(green)</b>	0.13	39.46	0.06	1.24	0.40	0.57	4.20	0.07	0.52	1.32	1.68	40.38	8.59	0.41	0.68
<b>8(white)</b>	0.02	71.17	0.06	2.24	2.90	3.28	6.52	0.02	0.51	0.02	0.02	0.03	11.38	0.56	0.73
<b>9(white)</b>	0.12	72.31	0.08	2.20	1.35	1.66	6.48	0.69	0.53	0.02	0.01	0.11	12.44	0.63	0.95
<b>10(white)</b>	0.12	68.59	0.01	2.51	10.09	0.59	8.82	0.21	0.35	0.02	0.03	0.01	7.15	0.44	0.48
<b>11(blue)</b>	0.07	73.84	0.10	2.32	0.93	0.75	5.82	0.06	0.65	0.16	0.07	0.28	11.34	0.55	1.08
<b>12(blue)</b>	0.08	72.63	0.10	2.55	1.43	0.78	7.22	0.41	0.81	0.10	0.02	0.24	11.64	0.61	0.91
<b>13(blue)</b>	0.12	70.51	0.04	2.79	0.01	0.59	8.12	0.99	1.14	0.06	0.01	0.02	13.33	0.88	0.85
<b>14(blue)</b>	0.14	66.93	n.d.	2.49	9.15	0.67	9.54	0.57	0.42	0.03	0.05	0.02	8.31	0.53	0.49
<b>14(white)</b>	0.12	66.73	n.d.	2.51	9.01	0.68	9.64	0.58	0.44	0.01	0.05	0.03	8.35	0.63	0.48
<b>15(white)</b>	0.14	69.06	0.03	2.65	5.54	0.79	8.15	1.25	0.42	0.01	0.01	0.05	10.03	0.75	0.38

Table 5.2 Major oxides (in wt%) measured by EMPA

Sample No.	P <sub>2</sub> O <sub>5</sub>	SiO <sub>2</sub>	TiO <sub>2</sub>	Al <sub>2</sub> O <sub>3</sub>	Sb <sub>2</sub> O <sub>3</sub>	MgO	CaO	MnO	FeO	CuO	SnO	PbO	Na <sub>2</sub> O	K <sub>2</sub> O	Cl
<b>16(white)</b>	0.08	71.54	0.09	2.27	1.61	1.94	6.76	1.87	0.57	0.07	0.02	0.18	11.06	0.56	0.86
<b>16(brown)</b>	0.14	65.45	0.07	2.31	1.84	1.83	6.71	4.50	0.67	0.26	0.27	0.71	13.11	0.78	0.61
<b>16(red)</b>	0.89	58.55	0.14	2.14	0.10	2.74	9.02	0.45	1.56	1.78	0.21	8.59	10.65	2.20	0.67
<b>16(black)</b>	0.15	65.03	0.16	2.46	n.d.	1.74	8.43	4.02	0.85	n.d.	0.13	n.d.	14.91	0.65	1.05
<b>17(white)</b>	0.08	69.70	0.10	2.23	2.22	1.95	6.81	1.82	0.57	n.d.	0.08	0	12.45	0.55	0.56
<b>17(brown)</b>	0.17	64.46	0.09	2.28	2.86	1.82	7.02	4.59	0.68	0.02	0.31	0.04	12.95	0.77	0.82
<b>17(red)</b>	0.72	62.90	0.18	2.27	0.10	2.51	9.01	1.59	1.48	n.d.	1.25	0.17	8.23	1.80	0.82
<b>17(black)</b>	0.17	65.10	0.17	2.46	n.d.	1.73	8.52	4.15	0.90	0.01	0.02	0.01	14.91	0.49	1.03
<b>18(white)</b>	0.03	68.42	0.05	2.06	4.13	2.53	6.77	0.87	0.40	0.01	0.08	0.01	12.65	0.53	0.78
<b>18(brown)</b>	0.13	65.83	0.09	2.30	1.47	1.88	6.66	4.62	0.72	n.d.	0.28	0.03	13.44	0.80	0.57
<b>18(red)</b>	0.90	58.33	0.16	2.10	0.13	2.75	9.00	0.45	1.59	n.d.	1.68	0.17	10.94	2.18	0.68
<b>18(black)</b>	0.14	64.45	0.16	2.44	0.01	1.79	8.38	4.32	0.92	n.d.	0.03	0.01	15.54	0.48	1.02
<b>19(green)</b>	0.09	70.06	0.08	2.31	0.76	0.67	6.24	0.24	0.59	1.53	0.08	3.53	11.65	0.66	1.01
<b>19(dark green)</b>	0.09	70.72	0.09	2.44	0.79	0.61	6.38	0.27	0.68	1.62	0.07	2.38	11.77	0.63	1.00
<b>19(black)</b>	0.56	64.20	0.14	2.27	0.27	2.16	7.51	3.90	1.11	0.02	0.03	0.03	15.28	1.33	0.78
<b>20(yellow)</b>	0.04	82.52	0.10	2.73	1.02	0.60	5.34	0.17	0.72	0.02	0.02	0.02	0.01	0.15	0.79
<b>20(black)</b>	0.14	68.58	0.10	2.36	0.62	1.07	7.34	3.46	0.77	0.01	0.04	0.01	13.30	0.67	1.02

## 5.4. LA-ICP-MS

In Figure 5.30, rare earth elements (REE) are displayed on a comparative spider graph. Samples No.4, No.7, No.13 and No.20 (black) are the most distinguishable. More precisely, sample No.20 (black area) presents the highest levels of most of the elements. The biggest difference of sample No.20 is observed in Ce. Samples No.1 and No.2 have also elevated levels of La. Samples No.7 and No.13 present the lowest concentration of many elements, especially La, Ce, Pr, Nd, Sm and Eu. The rest samples are quite homogeneous.

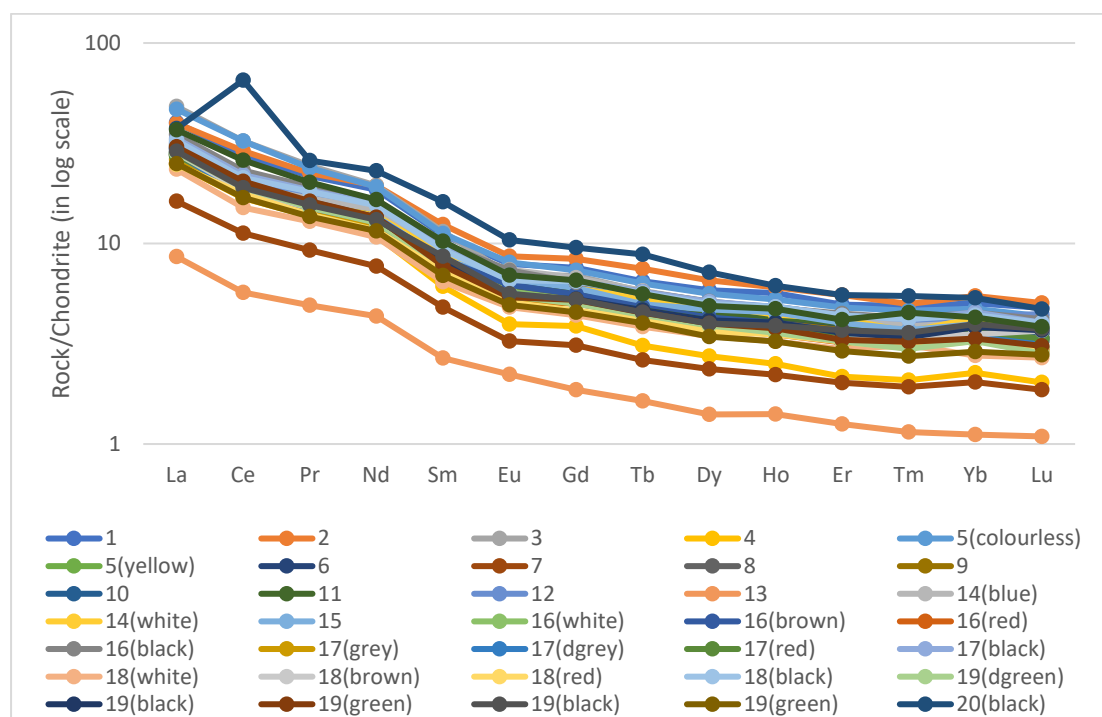


Figure 5.30 Chondrite-normalized (McDonough and Sun, 1995) trace element composition of the glass samples analyzed by LA-ICP-MS

Elements associated with the silica source, such as vanadium, chromium, zirconium, barium and tantalum are detected. Vanadium concentrations are between 4.18 and 95.1, Cr between 3.17 and 42.9, Zr 10.3 and 216, Ba 87.2 and 586 and Ta 0.02 and 0.4 ppm. Rubidium and strontium vary from 3.8 to 68.9, from 158 to 874 ppm respectively. Elements related to the colourants such as Ni and Zn can be found between 3.8 and 57.09 and 13.8 and 3509 ppm respectively.

The results of trace analyses of the glass artefacts are listed in Table 5.3 and Table 5.4

Table 5.3 Minor and trace elements (in ppm) measured by LA-ICP-MS

Sample No.	V	Cr	Co	Ni	Zn	Rb	Sr	Zr	Nb	Ag	Ba	La	Ce	Yb	Ta	Au
<b>1(red)</b>	23.12	18.09	6.82	17.70	454	10.30	723	85.20	3.08	21.30	296	9.51	16.71	0.81	0.20	0.16
<b>2(orange)</b>	38.20	39.80	14.89	47.30	3509	9.40	478	84.50	4.11	54.05	217	9.41	17.72	0.88	0.20	0.50
<b>3(red)</b>	25.20	17.90	27.19	57.09	269	40.20	403	64.20	2.80	69.20	249	11.42	19.91	0.68	0.19	0.60
<b>4(yellow)</b>	7.80	6.40	1.47	3.80	194	11.60	194	29.30	1.20	3.20	110	5.90	10.34	0.36	0.08	0.02
<b>5(colourless)</b>	26.17	15.50	13.14	17.50	68.20	26.40	476	48.50	1.80	25.70	359	11.07	19.92	0.76	0.12	0.12
<b>5(yellow)</b>	8.90	9.30	4.24	7.40	17.50	10.20	371	34.20	1.30	11.60	214	6.70	11.91	0.62	0.09	0.02
<b>6(green)</b>	10.50	9.30	4.05	6.70	33.40	12.30	400	50.40	1.70	4.030	192	7.15	12.40	0.57	0.10	0.09
<b>7(green)</b>	10.30	7.40	2.15	16.20	283	3.90	317	34.05	1.07	31.70	94.00	3.85	6.88	0.32	0.06	1.18
<b>8(white)</b>	9.80	9.90	1.69	5.12	48.70	9.00	409	50.00	1.60	0.60	182	5.56	11.15	0.56	0.09	0.03
<b>9(white)</b>	12.90	9.90	18.17	7.90	48.30	9.00	454	54.80	1.50	0.40	235	6.55	11.02	0.58	0.10	0.04
<b>10(white)</b>	7.60	10.12	4.81	5.06	22.15	6.70	423	36.60	1.15	0.30	261	6.69	11.29	0.64	0.08	0.02
<b>11(blue)</b>	10.70	11.70	9.55	9.08	178	8.60	362	60.00	2.10	4.90	171	7.34	12.56	0.63	0.14	0.17
<b>12(blue)</b>	14.30	12.80	373	18.40	39.80	9.30	454	62.40	1.90	1.60	219	7.51	13.08	0.69	0.12	0.10
<b>13(blue)</b>	4.18	3.17	95.53	4.50	13.80	4.20	158	10.30	0.30	0.03	87.2	2.03	3.50	0.18	0.02	n.d.
<b>14(blue)</b>	10.90	12.80	9.48	8.15	27.30	6.70	486	35.90	1.19	0.30	259	7.07	11.84	0.64	0.07	0.02
<b>14(white)</b>	10.80	11.70	8.83	8.05	29.15	6.80	468	35.09	1.12	0.30	249	6.66	11.20	0.68	0.07	0.03
<b>15(white)</b>	16.90	11.40	9.07	11.20	32.70	9.70	526	35.50	1.20	0.40	276	6.73	11.07	0.63	0.08	n.d.

Table 5.4 Continued from previous page

Sample N°.	V	Cr	Co	Ni	Zn	Rb	Sr	Zr	Nb	Ag	Ba	La	Ce	Yb	Ta	Au
<b>16(white)</b>	31.70	10.30	9.46	10.30	68.50	10.20	529	53.90	1.70	1.20	333	6.62	11.27	0.54	0.10	0.04
<b>16(brown)</b>	95.10	11.01	26.03	15.90	103	12.30	648	57.40	1.90	3.60	586	7.07	11.85	0.58	0.11	0.12
<b>16(red)</b>	20.17	16.01	10.75	15.90	439	8.30	596	54.40	2.30	10.30	272	5.95	11.16	0.53	0.15	0.08
<b>16(black)</b>	41.40	15.60	8.47	25.70	36.20	6.30	874	80.90	2.80	2.50	574	8.27	14.17	0.72	0.16	n.d.
<b>17(white)</b>	31.03	10.70	11.19	10.80	71.90	9.90	490	55.40	1.70	0.70	318	6.20	10.60	0.55	0.10	0.05
<b>17(brown)</b>	90.60	10.20	24.69	14.90	99.80	11.70	614	54.04	1.80	1.80	552	6.57	11.17	0.55	0.11	0.13
<b>17(red)</b>	22.20	17.70	11.09	17.30	486	9.19	648	57.80	2.50	12.80	297	6.48	12.02	0.59	0.17	0.09
<b>17(black)</b>	40.04	15.20	8.25	24.70	34.50	3.80	828	83.70	2.70	0.10	535	7.89	13.46	0.73	0.15	0.01
<b>18(white)</b>	24.80	8.90	6.29	6.60	73.10	8.50	417	44.50	1.40	0.80	227	5.55	9.26	0.44	0.08	0.05
<b>18(brown)</b>	91.00	10.90	25.11	15.30	98.50	12.40	616	55.50	1.80	1.90	551	6.70	11.28	0.56	0.11	0.11
<b>18(red)</b>	20.30	15.90	10.31	16.04	438	8.40	594	52.70	2.30	11.30	268	5.85	10.83	0.52	0.15	0.05
<b>18(black)</b>	40.10	14.90	8.09	25.20	33.30	3.80	817	80.60	2.60	0.13	537	7.71	13.01	0.50	0.15	0.00
<b>19(green)</b>	11.40	9.40	3.39	7.60	64.40	13.90	363	48.50	1.80	5.12	168	6.55	11.43	0.50	0.10	0.10
<b>19(dark green)</b>	12.60	9.90	3.53	8.07	438	14.90	401	49.13	1.80	5.50	180	6.74	11.62	0.52	0.10	0.10
<b>19(black)</b>	37.70	13.90	7.69	26.50	447	5.40	738	82.90	2.60	1.60	570	6.91	11.76	0.62	0.15	0.03
<b>20(yellow)</b>	14.30	20.70	2.84	5.90	49.50	18.40	351	81.90	2.90	4.03	168	8.75	15.93	0.69	0.18	0.05
<b>20(black)</b>	76.80	42.90	25.23	40.50	203	68.90	273	216	7.09	1.08	305	8.88	39.99	0.86	0.44	0.20

## 6. Discussion

### 6.1. Glass-making technology

The glass is composed mainly of silica, which is the network former. On the contrary, glass No.4 and No.7 are rich in PbO (33.19-40.38 wt%) with a low content of SiO<sub>2</sub> (39.46-41.05 wt%). This is an uncommon find, as there are only a few known examples for yellow colour (Mass et al., 1998) and no known cases for the green colour with so high concentrations of PbO. This high Pb content is more than the amount required for the formation of lead antimonate. As it has been proposed by Maltoni and Silvestri (2018) for orange glass, very high lead concentration might be explained by the presence of Pb in the primary batch.

The analysis of major and minor elements allows the grouping of the glass. Specifically, the ternary diagram of the normalized concentrations of Na<sub>2</sub>O, MgO + K<sub>2</sub>O and CaO has been used to determine the chemical glass type based on the flux. Figure 6.1 demonstrates that the analyzed glass samples are divided into two categories: natron soda-lime glass and plant-ashes soda-lime glass.

The only exception is sample No.20, which presents an uncommon low level of Na<sub>2</sub>O (0.01 wt%) in the yellow area. Although it could be an outlier, the combination of the low concentration of Na<sub>2</sub>O and the highest concentration of SiO<sub>2</sub> (82.52 wt%) among the samples suggest that de-alkalization could also be a reason for this composition. De-alkalization occurs when the glass is exposed to moisture, causing alkali ions in the glass network to be leached out and replaced by the hydrogen ions of water (Davison, 1989). According to data obtained by SEM-EDS, de-alkalization is evident in all the samples, but to a lesser extent.

According to Figure 6.1, all the brown (No.16, No.17, No.18), some of the red (No.3, No.16, No.17, No.18), some of the white (No.8, No.9, No.16, No.17), one orange (No.2), one yellow (No.4) and one black (No.19) glass belong to the plant-ashes soda-lime group. The rest samples are natron soda-lime glasses.

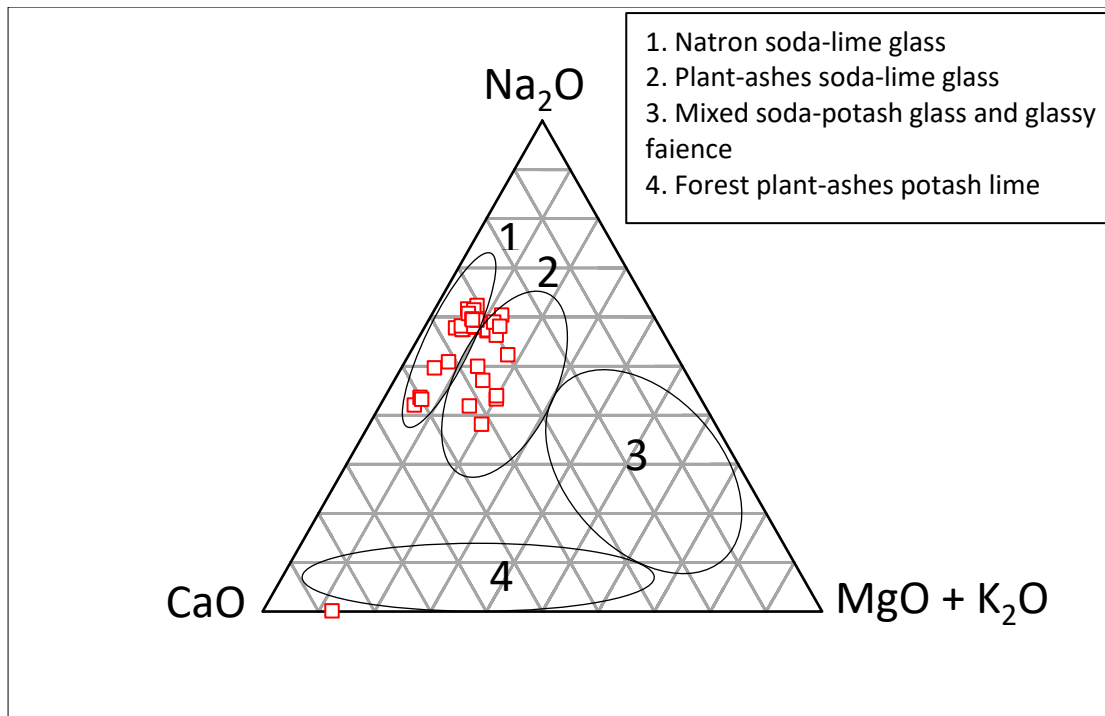


Figure 6.1 Ternary diagram of the normalized Na<sub>2</sub>O, MgO+K<sub>2</sub>O and CaO contents of all the glass samples analyzed by EMPA (Gratuze and Janssens, 2004)

Taking into consideration Figure 6.2, it is visible that only a part of the glass samples has the characteristic composition of natron glass, *i.e.*, K<sub>2</sub>O and MgO lower than 1.5 wt%, and P<sub>2</sub>O<sub>5</sub> approximately at 0.10 wt%. Elevated levels of K<sub>2</sub>O and MgO are detected in samples No.3, No.16 (red area), No.17 (red area) and No.18 (red area). These samples also have high concentration of P<sub>2</sub>O<sub>5</sub>, up to 0.9 wt%. This data is usually connected to the addition of plant ash. It is common to find Roman red, orange and yellow glass enriched in K<sub>2</sub>O and MgO, which could be connected to a particular production method. It is sometimes hypothesised that charcoal and fuel ashes were used as internal reducing agents in the production of these colours (Maltoni and Silvestri, 2018).

Samples No.8, No.9, No.16 (white and brown area), No.17 (white and brown area), No.18 (white and brown area) and No.19 (black area) have only high levels of MgO and low levels of K<sub>2</sub>O and P<sub>2</sub>O<sub>5</sub>. On the contrary of Figure 6.1, the low concentration of both K<sub>2</sub>O and P<sub>2</sub>O<sub>5</sub> exclude the use of plant ash. This elevated concentration of MgO could be attributed to recycling or mixing of various base compositions (Maltoni and Silvestri, 2018), to the use of a different source of antimony, containing some MgO, or of a silica-lime sand with dolomite (Verità et al., 2008).

Lastly, the relatively high content of Cl (0.77 wt% on average) is a further proof for the use of natron as a flux, as this mineral contains frequently high amounts of halite (NaCl).

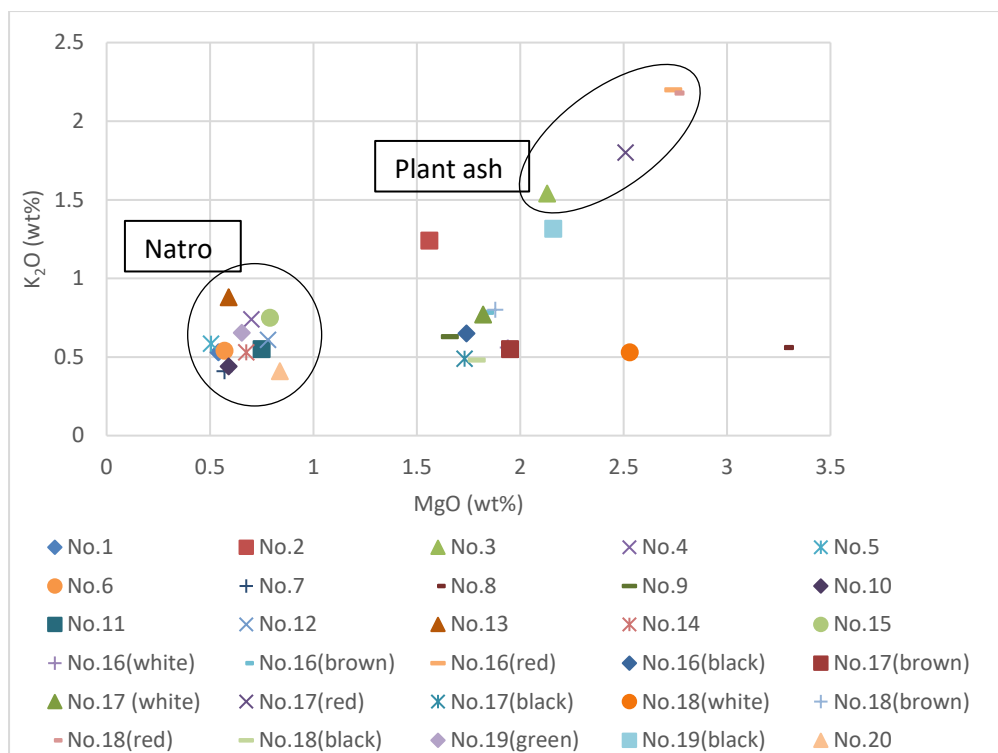


Figure 6.2 K<sub>2</sub>O vs MgO concentration (wt%) for all the analyzed samples by EMPA

## 6.1.1. Colourants and Decolourants

### 6.1.1.1. Red

The red samples, namely samples No.1, No.3, No.16 (red area), No.17 (red area) and No.18 (red area), are of the soda-lime-silica type. Figure 6.3 demonstrates that most of them, except No.1, have high K<sub>2</sub>O and MgO. This result, together with high P<sub>2</sub>O<sub>5</sub> levels, is normally explained by the use of plant ash as a flux. This is a peculiarity in comparison with the rest of the samples, but it is very common for Roman red glass (Henderson, 1991; Bandiera et al., 2020). It is a controversial issue, as many scholars attribute these values to the addition of charcoal as a reducing agent (Maltoni and Silvestri, 2018), whereas others to the use of a different fluxing agent (Verità and Santopadre, 2015; Bandiera et al., 2020).

All the red samples belong to the low Cu (0.06-1.82 wt%) and Pb (6.7-9.89 wt%) type (Freestone, 1987). Except sample No.1, they are rich in FeO ranging from 1.19 to 1.59 wt%, which indicates that iron was added intentionally as reducing agent. Indeed, red glass is generated by the reduction of the cupric oxide to cuprous Cu<sup>+</sup> ion. In this state, Cu can precipitate out as cuprite crystals (Cu<sub>2</sub>O) in the dendritic shape producing a glass known as sealing-wax red or the sub-micron metallic copper (Cu<sup>0</sup>) producing the so-called ruby-red (Bandiera et al., 2020). Both types of crystals function as colourants and as opacifiers. This is achieved by internal reducing agents and by having a strong reducing atmosphere during the whole process (Maltoni and Silvestri, 2018). Charcoal and metals such as Pb, Fe, Sb and Sn



have been proposed as reducing agents (Maltoni and Silvestri, 2018; Bandiera et al., 2020). Arletti et al. (2006) further highlights that the presence of Pb facilitates the precipitation of cuprite, whereas Fe is more suitable to generate metallic copper as stronger reducing conditions are required.

Sample No.1 has low concentration of FeO (0.53 wt%), which relates to the presence of Fe as a contaminant from the raw material (Schibille et al., 2012). The low Pb concentration is usually considered to give no actual benefit to the production of red colour and is attributed to tradition (Freestone, 1987). Nevertheless, it has also been supported that even low concentration of Pb facilitates the crystal growth, which increases the opacity and intensity of the colour (Freestone, 1987; Bandiera et al., 2020).

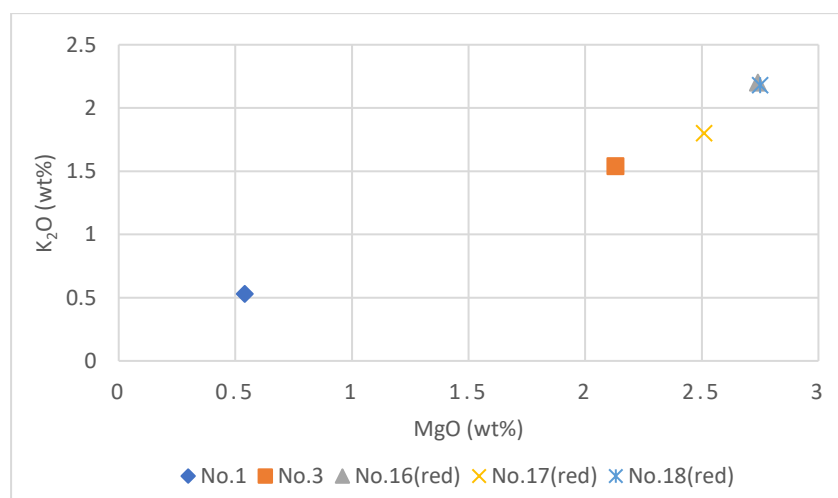


Figure 6.3 K<sub>2</sub>O vs MgO concentration (wt%) for the red glass (5) analyzed by EMPA

Sealing-wax red with high-copper (5-10 wt%) and high-lead (>10 wt%) was produced from the 4th century BC until the 1st century AD, when the ruby-red (low-copper (<5 wt%) and low-lead (<10 wt%)) appeared. Particles of metallic copper are precipitated during the cooling process through redox reactions and therefore there is no need for special heat treatment and careful control of the redox conditions of the furnace (Freestone, 1987; Bandiera et al., 2020). Therefore, this technique was less labor-intensive and less time-consuming.

Lastly, the positive correlation of Cu with Sn ( $r = 0.99$ ) suggests that Cu was added to the batch in the form of bronze (Degryse and Shortland, 2020). Accordingly, the positive strong correlation between Pb and Ag ( $r = 0.99$ ) shows that lead was added to the batch as litharge rather than scrap metal (Bandiera et al., 2019).

#### 6.1.1.2. Orange

Sample No.2, which is the only orange sample analyzed, is a natron-lime-silica glass. It has high concentration of Cu (8.32 wt%) and Pb (22.73 wt%). It

is also characterized by low levels of Na and high levels of Sb, Fe, and Sn which are also mentioned in other studies on orange glass (Ricciardi, 2009; Maltoni and Silvestri, 2018; Bandiera et al., 2020). These elements might be used to promote the nucleation of crystals which produce different hues (Bandiera et al., 2020). This data agrees with the data obtained for other orange *sectilia* (Verità et al., 2008; Santagostino Barbone et al., 2008; Tesser et al., 2020), but it cannot be fully representative for the Early Roman architectonic glass, due to the lack of samples.

The results suggest a production method for orange similar to that of sealing-wax red. They usually present the same high levels of Cu and Pb (Maltoni and Silvestri, 2008; Bandiera et al., 2020). The difference in the colour is probably due to finer-grained particles of  $\text{Cu}_2\text{O}$  (<400 nm) or the different morphologies of the crystallites (Brill and Cahill, 1988; Bandiera et al., 2020; Tesser et al., 2020). This is probably achieved through careful control of the redox condition during firing (Henderson, 1985).

#### 6.1.1.3. Yellow

Samples No.4, No.5 (yellow area) and No.20 (yellow area) are of the natron-lime-silica type with low levels of  $\text{K}_2\text{O}$  and  $\text{MgO}$ . The concentration of  $\text{SiO}_2$  ranges from 41.05 to 82.52 wt%. Low level of  $\text{SiO}_2$  for sample No.4 is explained by the high levels of Pb (33.19 wt%) which consequently lowers the concentration of  $\text{SiO}_2$ .

The yellow opaque colour is produced through the addition of lead antimonate ( $\text{Pb}_2\text{Sb}_2\text{O}_7$ ) or lead stannate ( $\text{Pb}_2\text{SnO}_4$ ) to the batch (Wainwright et al., 1986; Verità et al., 2013). The yellow areas of samples No.5 and No.20 have a relatively high concentration of Sb (1.02-1.13 wt%) and a low concentration of Sn (0.02-0.07 wt%) suggesting the use of lead antimonate as colourant and opacifier. On the contrary, sample No.4 seems to be produced through the addition of lead stannate due to the low levels of Sb (>0.4 wt%) and the high level of Sn (0.64 wt%).

#### 6.1.1.4. Green

Samples No.6, No.7 and No.19 (green area) are soda-lime-silica glasses, natron type. They have  $\text{SiO}_2$  concentration ranging from 39.46 to 73.46 wt%. The low level of  $\text{SiO}_2$  in sample No.7 is due to a high level of Pb (40.38 wt%).

Copper concentration ranges from 1.01 to 2.06 wt%, whereas the concentration of Pb, Sb and Sn ranges from 0.85 to 40.38 wt%, 0.40 to 0.85 and 0.05 to 1.68 wt%, respectively. Therefore, the green colour is produced from the addition of lead antimonate or lead stannate to a transparent Cu blue glass (Shortland, 2002; Arletti et al., 2006; Maltoni and Silvestri, 2018; Tesser et al., 2020). Samples No.6 and No.19 seem to be opacified through lead antimonate as the level of Sb surpasses 0.4 wt%, which shows a deliberate

addition (Brill and Cahill, 1988; Maltoni and Silvestri, 2018). On the contrary, the opacity of sample No.7 comes from the addition of lead stannate (Arletti et al., 2008), as it is rich in Sn (1.68 wt%).

The absence of correlation between Cu and Sn and between Cu and Zn may suggest that Cu was added to the batch in the form of metal copper or copper bearing minerals (Brill and Cahill, 1988).

#### 6.1.1.5. White

The composition of the white glass No.8, No.9, No.10, No.16 (white area), No.17 (white area) and No.18 (white area) is quite homogeneous. The concentration of SiO<sub>2</sub> ranges between 68.42 and 73.35, of Na<sub>2</sub>O between 7.15 and 12.89 and of CaO between 6.48 and 8.82 wt%.

White colour and the opacification derive from calcium antimonate (Ca<sub>2</sub>Sb<sub>2</sub>O<sub>7</sub> and CaSb<sub>2</sub>O<sub>6</sub>) (Lahlil et al., 2008) as shown by the positive correlation between Ca and Sb ( $r = 0.94$ ). The level of MgO is also very high, as previously observed for Roman white opaque glass. The high concentration of MgO has been attributed to the use of a source of antimony containing some MgO, of a silica-lime sand with dolomite (Verità et al., 2008), or to recycling (Maltoni and Silvestri, 2018). The absence of correlation between Sb and Mg excludes the provenance of Mg from the Sb source.

#### 6.1.1.6. Blue

The blue samples (No.11, No.12 and No.13) are quite homogeneous with silica concentrations ranging from 70.51 to 73.84, lime from 5.82 to 8.12 and soda from 11.34 to 13.33 wt%.

The blue colour is produced by the addition of Co in samples No.12 (373 ppm) and No.14 (9.48 ppm), whereas sample No.11 seem to be coloured also with the aid of Cu (0.16 wt%). The strong positive correlation between Cu and Zn ( $r = 0.99$ ) suggests that the copper was added in the form of brass, whereas the positive correlation between Co and Fe ( $r = 0.75$ ) that the cobalt came from an iron-rich ore. The high levels of Sb in samples No.11 and No.12 and of Mn in sample No.13 show that the glass was decolourized. Antimony could further contribute to the opacification of the glass.

#### 6.1.1.7. Cameo glass

The cameo glass samples (No.14 and No.15) are quite homogeneous. Silica concentration ranges from 66.73 to 69.06, that of soda between 8.31 and 10.03 and lime between 8.15 and 9.64 wt%.

In the literature, two categories of cameo glass are mentioned, *i.e.*, one with high Pb levels (>10 wt%) and one Pb-free (Bimson and Freestone, 1983). The glass samples from Lamia's Gardens have low PbO levels ranging from 0.02

to 0.05 wt%. All the points analyzed present high concentration of Sb (5.54-9.15 wt%) indicating the use of calcium antimonate as colouring and opacifying agent for the white glass (Bimson and Freestone, 1983). The blue glass is distinguishable by the relative high amount of both Cu (0.03 wt%) and Co (9.45 ppm), which could be connected to the use of both elements for the production of the blue colour.

#### 6.1.1.8. Brown

The brown areas of samples No.16, No.17 and No.18 are quite homogeneous as the silica concentration ranges from 64.46 to 68.58, soda from 12.95 to 13.44 and lime from 6.66 to 7.34 wt%.

It is worth mentioning the high concentration of Mn (4.42-4.62 wt%). The brown colour is produced by the addition of MnO into the batch (Caggiani et al., 2017). MgO could be related to the addition of MnO due to the elevated concentration and the positive correlation with MnO ( $r = 0.72$ ).

#### 6.1.1.9. Black

The black areas of samples No.16, No.17, No.18, No.19 and No.20 have a similar composition with the brown ones. They are quite homogeneous, with silica concentration ranging from 64.02 to 65.1, soda from 14.91 to 15.54 and lime from 7.51 to 8.52 wt%. The high concentration of Mn (3.9-4.32 wt%) into the batch, in conjunction with naturally occurring iron (concentration in range 0.77-1.11 wt%), suggests that the black glass belongs to the category of the black-appearing glass, where the real colour is deep purple, as discussed by Cagno et al. (2014) and Verità et al. (2008). This type of black glass has limited use during the 1st-2nd century AD. It is worth mentioning that the level of FeO is higher than in the brown glass, but not high enough to be considered an intentional addition.

#### 6.1.1.10. Decolourants

Maltoni and Silvestri (2018) distinguished four categories of glass, *i.e.*, the Mn-Roman glass with a concentration of MnO higher than 1 and Sb lower than 0.2 wt%, the Sb-Roman glass with level of Sb higher than 0.4 and of MnO less than 0.2 wt%, the Mn-Sb-Roman glass with both Mn and Sb above the natural occurring concentrations and the naturally coloured or coloured glass with both elements in low concentration.

Considering these categories, most of the samples analyzed belong to the mixed group with high concentration of both Sb and Mn ranging from 0.62 to 9.15 and from 0.41 to 4.62 wt% respectively. However, samples No.1, No.2, No.5 (yellow area), No.6, No.8, No.11, No.19 (green area) and No.20 (yellow area) have only high concentrations of Sb (0.64-1.13 wt%), whereas samples No.13, No.16 (black area), No.17 (red area), No.17 (black area), No.18 (black

area) and No.19 (black area) of Mn (0.99-4.32 wt%). No decolourants were found in samples No.3, No.4, No.7, No.16 (red area) and No.18 (red area).

A colourless areas of sample No.5 is worth special mention, as it is the only colourless glass analyzed. It seems that it is a naturally coloured glass, with low levels of antimony and manganese. Additionally, it presents the lowest level of Fe. The careful selection of Fe-poor raw materials could lead to a colourless glass even with low content of decolourants (Jackson, 2005; Silvestri et al., 2008).

Antimony was a very effective decolourant, as even a small amount could effectively neutralize FeO. On the contrary, the decoloring effect of Mn was efficient only with a ratio MnO/Fe<sub>2</sub>O<sub>3</sub> more than 2. Accordingly, only samples No.15, No.16 (white, brown and black areas), No.17 (white, brown and black areas), No.18 (white, brown and black areas) and No.19 (black area) seem to be adequately decolored with Mn. However, the high Mn content in the brown and black glass is, mainly, due to its intentional addition as a colourant.

The absence of correlation between Sb and Pb excludes a Sb-Pb mineral as raw material, pointing out the possible use of stibnite or an alloy (Rutten et al., 2009). The positive correlation between Mn and Ba ( $r = 0.80$ ) could suggest that Mn was introduced into the batch by psilomelane [(Ba, H<sub>2</sub>O) MnO<sub>5</sub>O<sub>10</sub>] rather than pyrolusite (MnO<sub>2</sub>) (Conte et al., 2014) (Figure 6.4).

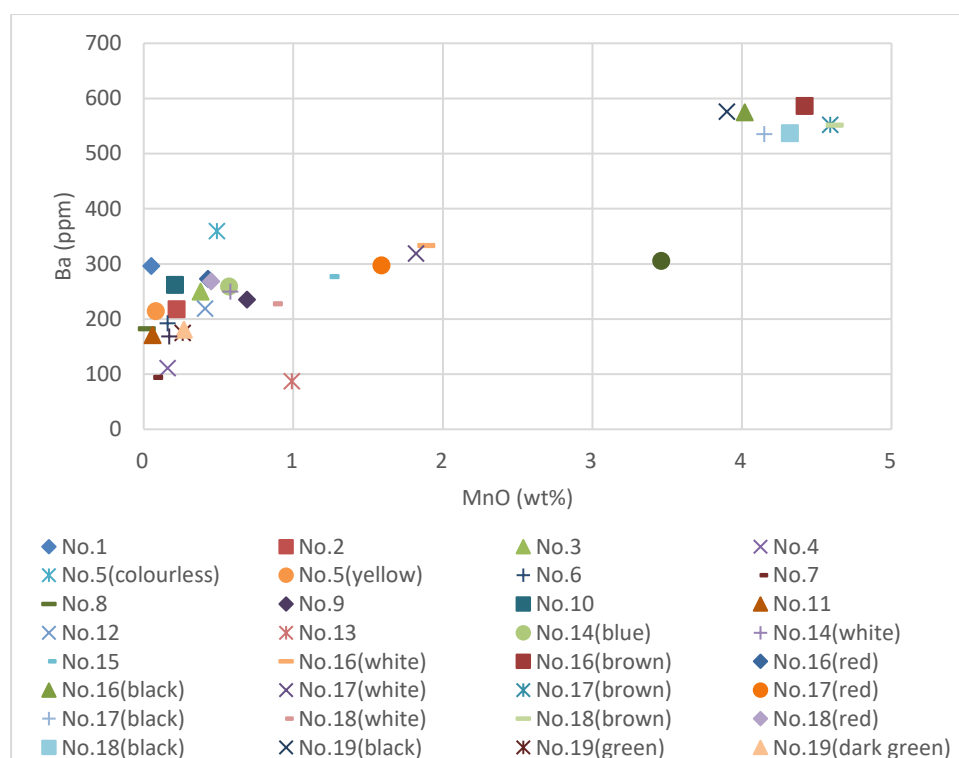


Figure 6.4 Ba vs MnO concentration (ppm/wt%) for all the samples, as collected by LA-ICP-MS and EMPA respectively

### 6.1.2. Opacifiers

Opacification is produced by tiny crystallites added to the batch as crystal powder or formed during the cooling process. Calcium antimonate ( $\text{Ca}_2\text{Sb}_2\text{O}_7$  and  $\text{Ca}_2\text{Sb}_2\text{O}_6$ ) or tin oxide ( $\text{SnO}_2$ ) were used as colourants and opacifiers for the white, turquoise and blue glass (Bimson and Freestone, 1983; Lahlil et al., 2008; Henderson, 2013). The strong positive correlation between Ca and Sb of the white ( $r = 0.94$ ), blue ( $r = 1$ ) and brown ( $r = 0.96$ ) opaque samples indicates the opacification by means of calcium antimonate.

On the contrary, lead antimonate ( $\text{Pb}_2\text{Sb}_2\text{O}_7$ ) or lead stannate ( $\text{Pb}_2\text{Sn}_2\text{O}_7$ ) produce yellow and green opaque glass (Wainwright et al., 1986; Verità et al., 2013). In this study, both chemical compounds are found in the yellow and green samples as discussed above.

There is a debate about the transition from the Sb-based opacifiers to the Sn-based ones. Although examples of prior use of Sn-based opacifiers are mentioned in the literature (Wainwright et al., 1986; Verità et al., 2013), it is often supported that the transition occurred during the 4th century AD (Henderson, 1991; Maltoni and Silvestri, 2018). Samples No.4 and No.7 are a further proof for the use of Sn-based opacifiers before the 4th century AD.

Some studies focus on the source of Sb in the opacifier. It is suggested that calcium antimonate was added through roasted stibnite. Stibnite was a well-known substance in Roman times due to its pharmaceutical use. Therefore, calcium antimonate was formed *in situ* through the reaction of added Sb with Ca already present in the batch (Mass et al., 1998; Shortland, 2002). As for lead antimonate, the high concentration of Pb in the yellow and green glass suggests the use of an Sb-rich source, such as litharge, which provided both Sb and Pb (Mass et al., 1998).

A distinct category includes red (No.1, No.3, No.16 (red area), No.17 (red area), No.18 (red area)) and orange (No.2) opaque glass, which were opacified through spherical microparticles of metallic copper ( $\text{Cu}^0$ ) or of cuprite oxide ( $\text{Cu}_2\text{O}$ ), respectively (Verità and Santopadre, 2015; Maltoni and Silvestri, 2018). The opacity in the glass is produced due to the dispersion of light (Freestone, 1987; Brill and Cahill, 1988).

Lastly, the concentration of Sb and Sn in the black samples (No.16, No.17, No.18, No.19 and No.20 black areas) is very low to suggest the intentional addition of an opacifier. Therefore, the opacification might have been achieved by the presence of crystals inside the glass matrix (Henderson, 1985; Arletti et al., 2008).

### 6.1.3. Recycling of glass

The use of broken glass into the glass production was common practice from the Flavian period onwards (Silvestri et al., 2008; Saguí, 2010). Concentrations higher than background levels for elements related to (de)colouring activities are considered proof of recycling. In this study, many samples have concentration between 100 and 1000 ppm of one to three of the following elements: Co, Cu, Zn, Sn, Sb and Pb (Figure 6.5). Only samples No.2, No.8, No.9, No.10 and No.15 do not have any of these elements between 100 and 1000 ppm.

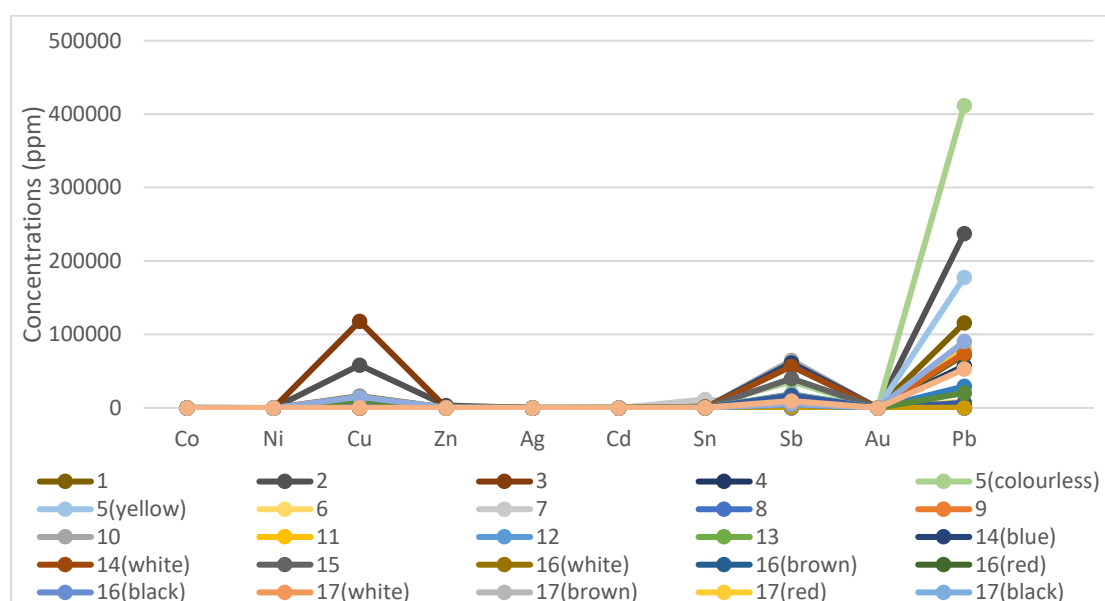


Figure 6.5 Plot of the elements related to recycling analyzed by LA-ICP-MS

Although these levels are still to be determined, when the concentration of elements such as Co, Ni, Cu, Zn, Ag, Cd, Sn, Sb, Au and Pb is between 100 and 1000 ppm, recycling is likely (Ceglia et al., 2019). Concentrations below 100 ppm indicate the use of recently produced glass, limited recycling or careful selection of the cullet (Silvestri et al., 2008). On the contrary, concentrations higher than 1000 ppm show intentional addition. Therefore, it can be assumed that at least a limited addition of recycled glass in the production of Lamia's Gardens architectonic glass was occurring.

Another indication of recycling is the decolourization with a mixture of Mn and Sb (Foster and Jackson, 2010; Freestone, 2015). If the mixture of Mn and Sb as decolourants is considered a proof for recycling, it could be supported that samples No.9, No.10, No.12, No.14, No.15, No.16 (white and brown areas), No.17 (white and brown areas), No.18 (white and brown areas) and No.20 (black area) might include recycled glass.



## 6.2. Provenance

Major, minor and trace element concentrations present an efficient method to investigate the provenance of the raw materials. As the silica source usually contains heavy minerals such as iron oxides, silicates and REE, it could be useful for provenance studies (Degryse and Shortland, 2020).

Taking into consideration the relatively high levels of  $\text{Al}_2\text{O}_3$  (1.24-3.23 wt%) and  $\text{CaO}$  (3.11-9.64 wt%), the use of a pure silica source like chert is excluded (Aerts et al., 2003). The obtained data suggests that the source of silica was an impure calcareous sand rich in feldspar.

Moreover, most of the samples have high Fe content ranging from 0.60 to 2.09 wt% (Schibille et al., 2012). Above that level, iron content is due to the intentional addition of a colourant. Samples No.1, No.5 (colourless area), No.7, No.8, No.9, No.10, No.14, No.15, No.16 (white area), No.18 (white area) and No.19 (green area) have a lower Fe content (<0.60 wt%). Lastly, the ratio between La and Yb is high ranging from 6.62 to 11.3 ppm indicating the use of an immature sand rich in light rare earth elements (Degryse and Shortland, 2020).

Furthermore, the concentration of Zr seems to be a reliable marker for differences in the silica source, usually introduced in the form of zircon, *i.e.*, a zirconium silicate ( $\text{ZrSiO}_4$ ). Its positive correlation with Ti is very strong ( $r = 0.80$ ). The low concentration of both elements is an indication that the sand used derives from a similar geological region (Aerts et al., 2003). Only samples No.2 and No.20 (black area) distinguish from the rest samples. Particularly for the Zr content, concentrations about 60 ppm are related to a Mediterranean beach sand, whereas higher concentrations about 160 ppm to inland sand (Silvestri et al., 2008). Most of the samples have low Zr content, that could be related to a Mediterranean sand including sample No.2. The only exception is sample No.20 (black area), that has a high Zr content (216 ppm).

Strontium in glass is a useful element to distinguish between coastal and inland sand. Most of the samples analyzed have high level of Sr (500 ppm on average) indicating the use of coastal sands rich in shell fragments, as lime source (Bugoi et al., 2018). Samples No.4 and No.13 are distinguishable as their Sr content is below 200 ppm indicating the use of limestone as lime source.

Concentrations of Ba can also contribute to the recognition of the sand used, because barium is related to alkali feldspars. In samples No.2, No.3, No.4, No.5 (yellow area), No.6, No.7, No.8, No.9, No.11, No.12, No.13, No.14 (white area), No.18 (white area), No.19 (green area), No.19 (dark green) and No.20 (yellow area), Ba is lower than 250 ppm and they were possibly produced with a sand relatively poor in alkali feldspars. For the rest samples, with



higher Ba (250-350 ppm), a sand richer in alkali feldspars is more likely. Concentrations above 350 ppm in samples No.5 (colourless area), No.16 (brown and black areas), No.17 (brown and black areas), No.18 (brown and black areas) and No.19 (black area) are also related to Mn, as they are introduced together with the mineral psilomelane.

The variations found in Sr, Ba and Zr content, together with the variable Ba/Sr ratio (Figure 6.6), allows one to assume that, apart from the use of a limestone for samples No.4 and No.13, at least two different sources of sand were used as a raw material for the production of the analyzed glass samples.

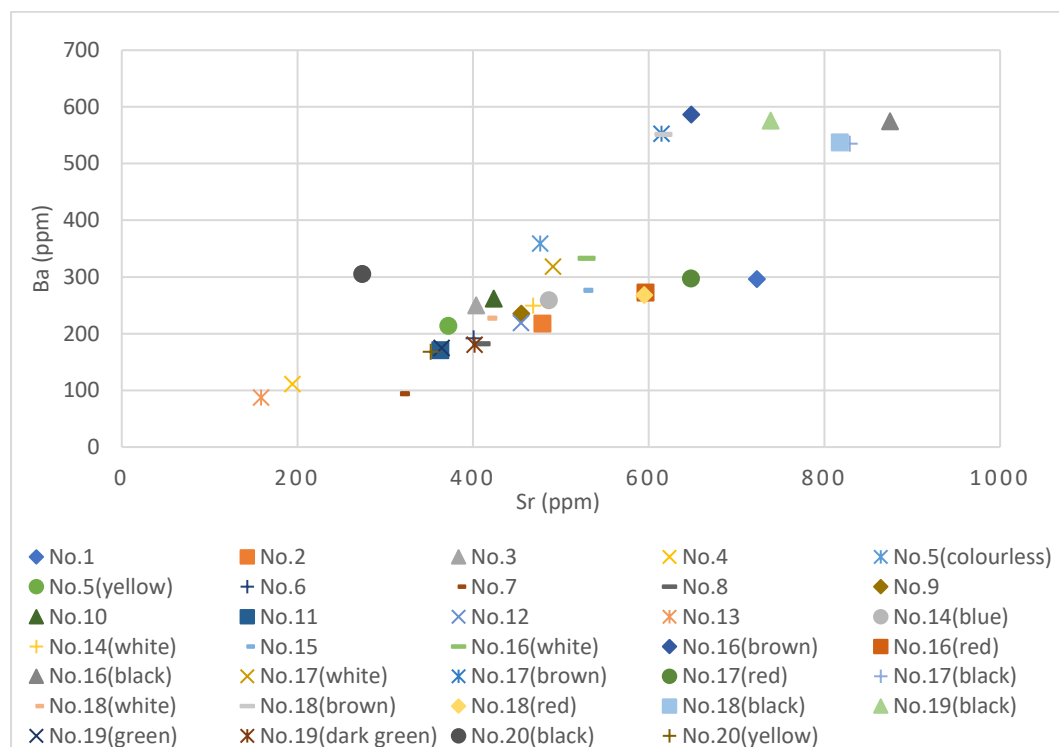


Figure 6.6 Ba vs Sr (ppm) for all the analyzed samples by LA-ICP-MS

Another indication for the use of two different silica sources is the  $TiO_2/Al_2O_3$  and  $Al_2O_3/SiO_2$  diagram, as it relates the elemental composition of the glass to the mineralogy of the glassmaking sands. In this system,  $SiO_2$  represents quartz,  $Al_2O_3$  feldspars and  $TiO_2$  heavy minerals (spinel or ilmenite) in the silica source (Schibille et al., 2017). Figure 6.7 shows that the ratio of Al and Si oxides is quite constant, whereas the ratio of Ti and Al oxides is variable, supporting the hypothesis of different silica sources. Following Schibille et al. (2017), a line can be drawn which indicate, mainly, two different silica sources. Specifically, the elements above the line belong to glass types usually related to Egyptian origin, whereas the rest samples seem to have Levantine origin.

The only sample that really stands out is sample No.2, which could point to a different production center. It has been already proposed that the sealing-wax red glass was produced in different primary centers (Henderson, 2013). This

could also apply to the orange glass in the present study, having similar chemical composition.

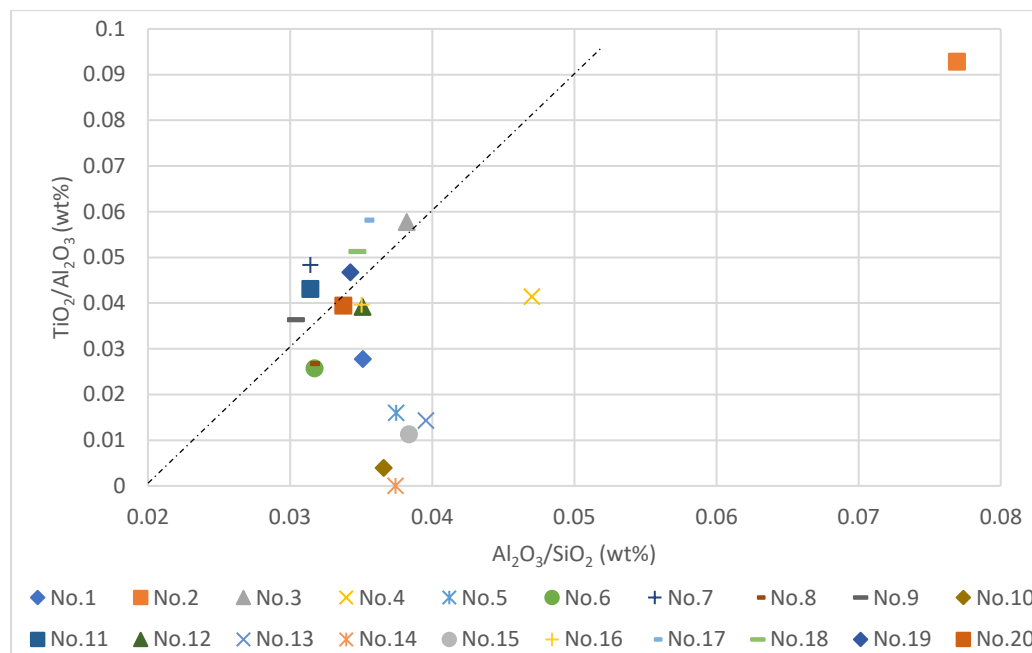


Figure 6.7  $TiO_2/Al_2O_3$  vs  $Al_2O_3/SiO_2$  (wt%) for all the analyzed samples by EMPA (Schibille et al., 2017)

As specific provenance is more commonly reported for Roman glass of the 4th century AD onwards, a comparison between the glass samples analyzed in this study and the data provided by Ceglia et al. (2019) for Late Roman glass will be attempted to distinguish between Levantine and Egyptian sources of sand.

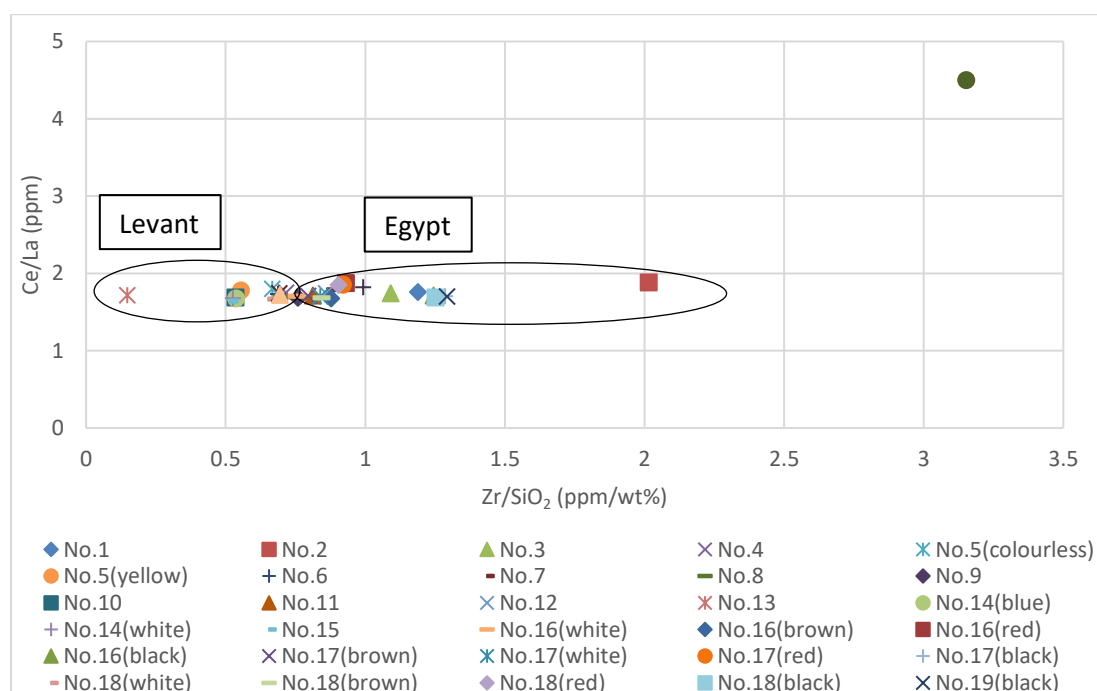


Figure 6.8 Concentration ratio of Ce/La (ppm) vs  $Zr/SiO_2$  (ppm/wt%) for all the samples analyzed by EMPA and LA-ICP-MS (compared to Ceglia et al., 2019)

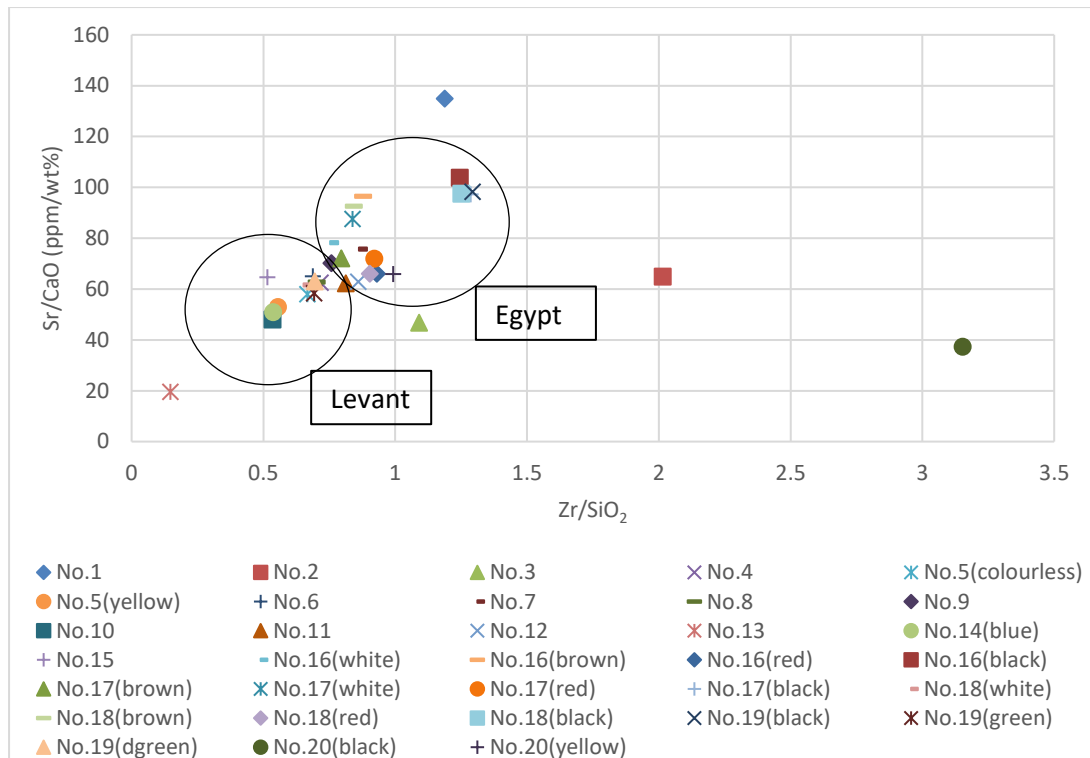


Figure 6.9 Concentration ratio of Sr/CaO vs Zr/SiO<sub>2</sub> (ppm/wt%) for all the samples analyzed by EMPA and LA-ICP-MS (compared to Ceglia et al., 2019)

The high similarity between the major composition of the glass samples supports the hypothesis that only a few production centers of raw glass, located in the Eastern Mediterranean, existed in the Roman Empire (Fontaine and Foy, 2007).

According to Figure 6.8 and Figure 6.9, there could be a distinction between two different known sand sources. The first category of glass, that has similar characteristics with the glass categories normally attributed to Egypt, has higher Sr/CaO and Zr/SiO<sub>2</sub> ratios indicating a sand source richer in Sr and Zr than the second category, normally attributed to sand from Levantine coast. The Ce/La ratio is constant showing that the sand has the same low degree of maturity. The only sample that distinguishes in both figures is No.20 (black area). In Figure 6.9 samples No.1 and No.2 also distinguish. This means that they were made from sand with the same level of maturity but probably from a different geographical region.

## 7. Conclusion

The multi-analytical approach used to investigate the architectonic glass found in Lamia's Gardens allowed the characterisation of several crucial aspects of this glass, providing valuable information on its production technology and provenance. The glass material was examined by optical microscopy, SEM-EDS, EMPA and LA-ICP-MS.

All the glasses analyzed belong to the natron-lime-silica type. As natron-lime-silica glass was the most common glass type produced during Roman imperial times, architectonic glass was no exception. The elevated concentration of  $K_2O$ ,  $MgO$  and  $P_2O_5$  observed in the red *sectilia* can be explained by the addition of fuel ash in a natron glass as reducing agent, whereas the elevated concentrations of  $MgO$  found in the white and brown samples must be related to the production of colour.

The glass samples analyzed consist of a variety of colours. The red glass belongs to the type known as ruby-red, which was a Roman invention and was widespread from the second half of the 2nd century AD onwards. It is characterized by low concentrations of  $Cu$  and  $Pb$ . On the contrary, the orange glass is a high-copper, high-lead glass. Accordingly, the composition of the red and orange glass is similar. The difference in colour was due to the size of the particles.

The yellow colour is produced through the addition of lead antimonate or lead stannate to a colourless glass. Green also is imparted through the addition of these compounds to a Cu blue glass. The chronological range of use of these colourants is a controversial issue. Lead stannate is considered to be extensively used from the 4th century AD onwards. Therefore, the glass samples from Lamia's Gardens are evidence for its earlier use.

Similarly, the white glass was produced by the addition of calcium antimonate, which is the common colourant for white glass. The blue glass was coloured by the addition of  $Co$ , or the combination of  $Co$  and  $Cu$ .

As for the brown and black glass, they have similar composition. Their main colourant is manganese giving them a purple hue. The difference in colour must be due to the difference in the concentration of  $Fe_2O_3$ .

Most of the glass samples are decolourized as it is evident by the presence of  $Sb$ ,  $Mn$  or both. Most of them are decolourized by the combination of  $Sn$  and  $Mn$ . The only colourless area analyzed (No.5) seem to be produced by the careful selection of the raw materials, as the concentration of  $Fe$  is very low.  $Sb$  seems to be added in the form of roasted stibnite, whereas  $Mn$  as psilomelane.

The opacification is achieved through the addition of an opacifying agent or the morphology of the particles. Accordingly, calcium antimonate is added to produce white, blue and brown opaque glasses, whereas lead antimonate or lead stannate to produce green and yellow opaque glasses. On the contrary, opacity in the red and black glasses is achieved through the morphology of the particles.

As for recycling, the existence of glasses decoloured by both Sb and Mn could suggest that some of the glass samples are recycled. The indication for recycling related to the colourants is a further proof for the addition of recycled glass into the batch.

Lastly, based on the concentrations of Zn, Sr and Ba, at least two sand sources can be hypothesized. The comparison between the glass samples analyzed and previous data for Egyptian and Levantine glass from the 4th century AD onwards could indicate that the glass fragments found in Lamia's Gardens could derive from the same locations as late Roman glass. Nevertheless, attention must be paid as the data compared belong to different chronologies.

Therefore, the multi-analytical approach applied contributed to address the research questions. The lack of comparative studies on architectonic glass of the 1st century AD sets considerable limitations regarding the interpretation of the data. In this view, this study could be considered as a preliminary endeavour on the technology and provenance of early Roman architectonic glass.

A further step would be to study a higher number of architectonic glass samples found in Lamia's Gardens for more representative data. Moreover, this study could be extended towards other significant archaeological sites to verify and improve our interpretation, or to other types of glass, such as vessels, found in Lamia's Gardens.

## Bibliography

Aerts, A., Janssens, K., Velde, B., Adams, F. and Wouters, H., "Analyses of the composition of glass objects from Qumran, Israel", in: Nenna, M.D. (eds.), 2000, 113-121

Aerts, A., Velde, B., Janssens, K., Dijkman, W., "Change in silica sources in Roman and post-Roman glass", *Spectrochimica Acta, Part B*, Vol.58, 2003, 659-667

Alagia, D., "Topografia degli Horti Lamiani. Riconsiderazioni di un tema archeologico", *Scienze dell'Antichità*, Vol.20 (1), 2014, 247-266

Albertoni, M., "La necropoli esquilina arcaica e repubblicana", *Roma Capitale*, 1983, 140-155

Arletti, R., Quartieri, S., Vezzalini, G., "Glass mosaic tesserae from Pompeii: an archaeometrical investigation", *Mineral*, Vol.75, 2006, 25-38

Arletti, R., Quartieri, S., Vezzalini, G., Sabatino, G., Triscari, M., Mastelloni, M.A., "Archaeometrical analyses of glass cakes and vitreous mosaic tesserae from Messina (Sicily, Italy)", *Journal of Non-Crystalline Solids*, Vol.354, 2008, 4962-4969

Bandiera, M., Lehuédé, P., Verità, M., Alves, L., Biron, I., Vilarigues, M., "Nanotechnology in Roman Opaque Red Glass from the 2nd Century AD. Archaeometric Investigation in Red Sectilia from the Decoration of the Lucius Verus Villa in Rome", *Heritage*, Vol.2, 2019, 2597-2611

Bandiera, M., Verità, M., Lehuédé, P., Vilarigues, M., "The technology of copper-based red glass sectilia from the 2nd Century AD Lucius Verus Villa in Rome", *Minerals*, Vol.10, 2020

Barag, D., *Catalogue of the western Asiatic glass in the British Museum*, Vol.1, 1985

Barbera, M., Barrano, S., De Cola, G., Festuccia, S., Giovannetti, L., Menghi, O., Pales, M., "La villa di Caligola. Un nuovo settore degli Horti Lamiani scoperto sotto la sede dell'ENPAM a Roma", *The Journal of Fasti Online*, 2010

Barbera, M., "Gli Horti Lamiani: topografia e organizzazione del complesso, alla luce dei vecchi e nuovi scavi", in: Ghini, G. (eds.), *Caligola. La trasgressione al potere, Catalogo della Mostra (Nemi, 2013)*, 2013, 179-188

Barrano, S., Martines, M., "Via Ariosto. Un contributo per la conoscenza della topografia antica dell'Esquilino", *The Journal of Fasti Online*, 2006

Barrano, S., Colli, D., Martines, M., "Piazza Vittorio Emanuele II. Un nuovo settore degli Horti Lamiani", *The Journal of Fasti Online*, 2007

- Bellintani, P., "Frattesina, l'ambre e la produzione vitrea nel contesto delle relazioni transalpine", *Ori delle Alpi*, 1997, 117-133
- Bertoletti, M., Cima, M., Talamo, E., *Centrale Montemartini. Musei Capitolini*, 2007
- Bimson, M., Freestone, I.C., "An analytical study of the relationship between the Portland vase and other Roman cameo glasses", *Journal of Glass Studies*, Vol.25, 1983, 55-64
- Boschetti, C., "Vitreous Materials in Early Mosaics in Italy: Faience, Egyptian Blue, and Glass", *Journal of Glass Studies*, Vol.53, 2011, 59-91
- Braidwood, J., *Excavations in the plain of Antioch*, 1960
- Brill, R., "Scientific Studies of the Panel Materials", in: Ibrahim, L., Scranton, R., Brill, R. (eds.), *Kechreai, Eastern Port of Corinth*, Vol.2, 1976, 227-255
- Brill, R.H., "Scientific investigation of the Jalame glass and related finds" in: Weinberg, G.D. (eds.), *Excavations at Jalame: site of a glass factory in late Roman*, 1988, 257-294
- Brill, R.H., Cahill, N.D., "A red opaque glass from Sardis and some thoughts on red opaques in general", *The Journal of Glass Studies*, Vol.30, 1988, 16-27
- Brill, R.H., Whitehouse, D., "The Thomas Panel", *Journal of Glass Studies*, Vol.30, 1988, 34-50
- Bugoi, R., Alexandrescu, C., Panaite, A. "Chemical composition characterization of ancient glass finds from Troesmis – Turcoaia, Romania", *Archaeological Anthropological Science*, Vol.10, 2018, 571-586
- Caggiani, M., Mangone, A., Mastrorocco, F., Taccogna, C., Laviano, R., Giannossa, L., "The Tetris game of scientific investigation. Increase the score embedding analytical techniques. Raw materials and production technology of Roman glasses from Pompeii", *Microchemical Journal*, Vol.131, 2017, 21-30
- Cagno, S., Cosyns, P., Izmer, A., Vanhaecke, F., Nys, K., Janssens, K., "Deeply colored and black-appearing Roman glass: a continued research", *Journal of Archaeological Science*, Vol.42, 2014, 128-139
- Ceglia, A., Cosyns, P., Schibille, N., Meulebroeck, W., "Unravelling provenance and recycling of late antique glass from Cyprus with trace elements", *Archaeological Anthropological Science*, Vol.11, 2019, 279-291
- Cicero, M.T., *Cicero's Letters to Atticus*, Translated by D.R. Shackleton-Bailey, Vol.1, Books 1-2, 2004
- Cima, M., La Rocca, E., "Le tranquille dimore degli dei. La residenza imperiale degli Horti Lamiani", *Catalogo della mostra*, 1986

- Cima, M., La Rocca, E., "Horti Romani", Atti del Convegno internazionale, BullCom, Vol.6, 1998
- Cima, M., Talamo, E., Gli Horti di Roma antica, 2008
- Coarelli, F., "Campus Esquilinus", Lexicon Topographicum Urbis Romae I, 1993, 218-219
- Conte, S., Chinni, T., Arlettic, R., Vandinid, M., "Butrint (Albania) between eastern and western Mediterranean glass production: EMPA and LA-ICP-MS of late antique and early medieval finds", Journal of Archaeological Science, Vol.49, 2014, 6-20
- Cosyns, P., Janssens, V. Van der Linen, Schalm, O., "Black glass in the Roman Empire: A work in progress", in: Creemers, G., Demarsin B, Cosyns P. (eds), Roman glass in Germania Inferior. Interregional comparisons and recent results. Proceedings of the International conference (Tongeren 2005), 2006, 30-41
- Cursi, G., "Roman Horti: A topographical view in the Imperial era, public/private". An exhibition of the Q-Kolleg at the Winchelmann-Institut Humboldt-Universität zu Berlin in cooperation with the Dipartimento Scienza dell'Antichità of the Sapienza-Università di Roma (19/06/2019-31/12/2019), 2019, 124-140
- Davison, S., Conservation and restoration of glass, 1989
- Degryse, P., Glass Making in the Greco-Roman World, 2014
- Degryse, P., Scott, R.B., Brems, D., "The archaeometry of ancient glassmaking: reconstructing ancient technology and the trade of raw materials", Perspective, Vol.2, 2014, 224-238
- Degryse, P., Shortland, A.J., "Interpreting elements and isotopes in glass: A review", Supplement: Isotopes in Archaeometry, Vol.62, 2020, 117-133
- Fontaine, S.D., Foy, D., "L'épave Ouest-Embiez 1, Var: le commerce maritime du verre brut et manufacture en Méditerranée occidentale dans l'Antiquité", in: Revue archéologique de Narbonnaise, Vol.40, 2007, 235-265
- Dussart, O., Le verre en Jordanie du Sud, 1998
- Flowers, T., Hajibagheri, M., Clipson, N., "Halophytes", The Quarterly Review of Biology, Vol.61, 1986, 313-337
- Foster, H.E., Jackson C.M., "The composition of "naturally coloured" late Roman vessel glass from Britain and the implications for models of glass production and supply", Journal of Archaeological Science, Vol.36, 2010, 189-204



- Freestone, I., "Composition and Microstructure of Early Opaque Red Glass", *British Museum Occasional Paper*, Vol.56, 1987, 173-191
- Freestone, I., "Looking into glass", *Science and the past*, 1991, 37-56
- Freestone, I., "Chemical analysis of "raw" glass fragments", *Excavations at Carthage*, Vol.2, 1, 1994
- Freestone, I., Gorin-Rosen, Y., Hughes, M.J., "Primary glass from Israel and the production of glass in late antiquity and the early Islamic period", in Nenna, M.D. (eds.), 2000, 65-84
- Freestone, I., Wolf, S., Thirlwell, M., "The production of HIMT glass: elemental and isotopic evidence", *Annales of the 16th Congress of the International Association for the History of Glass*, 2005, 153-157
- Freestone, I., "The recycling and reuse of Roman glass: Analytical approaches", *Journal of Glass studies*, Vol.57, 2015, 29-40
- Gallo, F., Silvestri, A., Degryse, P., Ganio, M., Longinelli, A., Molin, G., "Roman and late-Roman glass from north-eastern Italy: The isotopic perspective to provenance its raw materials", *Journal of Archaeological Science*, Vol.62, 2015, 55-65
- Ganio, M., Boyen, S., Fenn, T., Scott, R., Vanhoutte, S., Gimeno, D., Degryse, P., "Roman glass across the Empire: an elemental and isotopic characterization", *Journal of Analytical Atomic Spectrometry*, Vol.27, 2012, 743-753
- Gliozzo, E., Santagostino Barbone, A., D'Acapito, F., Turchiano, M., Turbanti Memmi, I., Volpe, G., "The sectilia panels of Faragola (Ascoli Satriano, Southern Italy): A multi-analytical study of the green, marbled (green and yellow), blue and blackish glass slabs", *Archaeometry*, Vol.52 (3), 2010, 389-415
- Gorin-Rosen, Y., "The ancient glass industry in Israel: Summary of the finds and new discoveries", in: Nenna, M.D. (eds.), 2000, 49-64
- Gratuze, B., Barrandon, J.N., *Islamic glass weights and stamps: analysis using nuclear techniques*, *Archaeometry*, Vol.32, 1990, 155-162
- Gratuze, B., Janssens, K., "Provenance analysis of glass artefacts", *Comprehensive Analytical Chemistry*, Vol. 42, 2004, 663-712
- Grose, D.F., *The Toledo Museum of Art. Early ancient glass. Core-formed, rod-formed, and cast vessels and objects from the late Bronze age to the early Roman Empire, 1600 B.C. to A.D. 50*, 1989
- Guidobaldi, F., "Les résidences impériales de Rome en dehors du Palatin, Rome et ses palais", *Dossiers de l'Archéologie*, Vol.336, 2009, 76-79

- Guimier-Sorbets, A.M., "Les ateliers de mosaïstes à Alexandrie à l'époque hellénistique et au début de l'époque impériale: Continuité et innovation", in: Paunier, D., Schmidt, C. (eds.), VIIIème Colloque International sur la Mosaïque Antique, 2001, 281-297
- Guspini, L., "Nuovi ritrovamenti in Via Ariosto sull'Esquilino", *The Journal of Fasti Online*, 2007
- Harden, D.B., "Ancient glass I: pre-Roman", *The Archaeological Journal*, Vol.125, 1968, 46-72
- Häuber, C., "I vecchi ritrovamenti (prima del 1870)", in: Cima, M., La Rocca, E. (eds.), 1986, 167-17
- Henderson, J., "The raw materials of early glass production", *Oxford Journal of Archaeology* 4 (3), 1985, 267-291
- Henderson, J., "The scientific analysis of ancient glass and its archaeological interpretation", *Scientific analysis in archaeology and its interpretation*, 1989, 30-62
- Henderson, J., "Chemical characterisation of Roman glass vessels, enamels and tesserae", *Materials issues in art and archaeology II, Research Society Symposium Proceedings*, Vol.185, 1991, 601-607
- Henderson, J., *The science and archaeology of materials*, 2000
- Henderson, J., *Ancient Glass: An Interdisciplinary Exploration*, 2013
- Hodges, H., *Artifacts: An Introduction to Early Materials and Technology*, London, 1981.
- Ignatiadou, D., "Research on the nitrum chalestricum", *Archaeological Work in Macedonia and Thrace*, Vol.16, 2002, 241-248
- Ignatiadou, D., Dotsika, E., Kouras, A., Maniatis, Y., "Nitrum chalestricum : the natron of Macedonia", in : Nenna, M.D. (eds.), *Annales de 16e Congrès de l'association internationale pour l'histoire du verre*, 2004, 64-67
- Israeli, Y., "What did Jerusalem's first-century BCE glass workshop produce?", in: Nenna, M.D. (eds.), *Annales du 16e Congrès de l'association Internationale pour l'Histoire du verre*, 2005, 54-58
- Jackson C.M., Baxter, M.J., Cool, H.E.M., "Identifying group and meaning: An investigation of Roman colourless glass", in Foy, D., Nenna, M.D. (eds.), *Échanges et commerce du verre dans le monde antique (colloque de l'AFAV, Aix-en-Provence, Marseille 2001)*, *Monographies Instrumentum*, Vol.24, 2003, 33-39
- Jackson, C.M., "Making colourless glass in the Roman period", *Archaeometry*, Vol.47 (4), 2005, 763-780

- Jackson-Tal, R.E., "The late Hellenistic glass industry in Syro-Palestine: A reappraisal", *Journal of Glass Studies*, Vol.46, 2004, 11-32
- Janssens, K., *Modern Methods for Analysing Archaeological and Historical Glass*, Vol.1, 2013
- Kowatli, I., Curvers, H.H., Stuart, B., Sablerolles, Y., Henderson, J., Reynolds, P., "A pottery and glassmaking site in Beirut (015)", *Bulletin de Archéologie et d' Architecture Libanaises*, Vol.10, 2008, 103-120
- Lahlil, S., Biron, I., Galois, L., Morin, G., "Rediscovering ancient glass technologies through the examination of opacifier crystals", *Applied Physics A*, Vol.92 (1), 2008, 109-116
- Lanciani, R., *Ancient Rome in the Light of Recent Discoveries*, 1888
- Lanciani, R., *Forma Urbis Romae*, 1893
- Lanciani, R., *Fascino di Roma antica*, 1986
- Lazzara, A., *Analisi archeobotaniche dei resti di epoca romana rinvenuti nello scavo di Piazza Vittorio Emanuele II, Roma*, Master thesis, 2019
- Lemke, C., "Reflections of the Roman Empire: The first-century glass industry as seen through traditions of manufacture", *The prehistory and history of glassmaking technology* (ed. P. McCray), *Ceramics and Civilization*, Vol.8, 1998, 269-292
- Mallowan, M.E.L., "Excavations at Tell Brak and Chagar Bazar", *Iraq*, Vol.9, 1947, 1-259
- Maltoni, S., Silvestri, A., "Innovation and tradition in the fourth century mosaic of the Casa delle Bestie Ferite in Aquileia, Italy: archaeometric characterization of the glass tesserae", *Archaeological Anthropological Science*, Vol.10, 2018, 415-429
- Mass, J., Stone, R., Wypyski, M., "The mineralogical and metallurgical origins of Roman opaque coloured glasses", in: McCray, P., Kingery, W.D. (eds.), *The prehistory and history of glassmaking technology*, *Ceramics and Civilisation*, VIII, 1998, 121-144
- Matson, F.R., "The composition and working properties of ancient glass", *The Journal of Chemical Education*, Vol.28, 1951, 82-87
- McDonough, W.F., Sun, S., "The composition of the Earth", *Chemical Geology*, Vol.120, 1995, 223-253.
- Menghi, O., *Piazza Vittorio, proprietà Madi S.r.l. Carotaggi a scopo di ricerca archeologica, relazione scientifica (sondaggi 1-43), maggio-giugno: 1-32 (prot. SAR n.d.)*, 2002

- Menghi, O., Piazza Vittorio, proprietà Madi S.r.l. Carotaggi a scopo di ricerca archeologica, relazione scientifica (sondaggi 44-117), aprile 2003-febbraio 2004 (prot. SAR n° 9542/30.IV.2004), 2004
- Menghi, O., Piazza Vittorio, proprietà Madi S.r.l. Carotaggi a scopo di ricerca archeologica, relazione scientifica (sondaggi 118-136), dicembre 2004-gennaio 2005 (prot. SAR n° 1138/21.I.2005), 2005
- Morel, J., Amrein, H., Meylan, M.F., Chavalley, C., "Un atelier de verrier du milieu du 1er siècle après J-C a Avenches", *Archéologie der Schweiz*, Vol.15, 1991, 2-17
- Morricone, M.L., "Edificio sotto il tempio di Venere e Roma", *Studi per Laura Breglia*, v.3, *Archeologia e storia*, supplement no.4 to *Bollettino di Numismatica*, 1987, 69-82
- Nenna M.D., Vichy, M., Picon M., "L'atelier de verrier de Lyon, du 1er siècle après J-C, et l'origine des verres « Romains »", *Revue d'Archéométrie*, Vol.21, 1997, 81-87
- Nenna, M.D., *Les ateliers de verriers dans le monde grec aux époques classique et hellénistique*. Topoi, 1998, 693-701
- Nenna, M.D., *La Route du verre: Ateliers primaires et secondaires du second millénaire av. J.-C. au Moyen Age*, 2000
- Nenna M.D., Picon, M., Thirion-Merle, V. and Vichy, M., "Ateliers primaires du Wadi Natrun: Nouvelles découvertes", in : Nenna, M.D. (eds.), *Annales of the 16e Congres de l'Association Internationale pour l'Histoire du Verre*, 2005, 59-63
- Nibby, A., *Roma nell'anno MDCCCXXXVIII*, Vol. II, 1838
- Nicholson, P.T., *Brilliant things for Akhenaten. The production of glass, vitreous materials and pottery at Amarna site 045.1*, 2007
- Nolte, B., "Die Glasgefäße im alten Ägypten", Berlin: *Münchener Ägyptologische*, Vol.14, 1968
- Oppenheim, A.L., "Towards a History of Glass in the Ancient Near East", *Journal of the American Oriental Society*, Vol.93, 1973, 259-266
- Paolucci, F., "Architettura e scultura negli horti romani: Il giardino antico da Babilona a Roma", 2007, 72-83
- Paynter, S., "Analyses of colourless Roman glass from Binchester, County Durham", *Journal of Archaeological Science*, Vol.33, 2006, 1037-1057
- Petsas, P., "Mosaics from Pella", *Colloque international sur la mosaïque gréco-romaine* (Paris, August 29-September 3, 1963), 1965, 41-56
- Philo, *Legatio ad Gaium*, Translated by M. Smallwood, Leiden, 1961

- Pichou, J.L., Pouchoir, F., "PAP procedure for improved quantitative microanalysis", *Microbeam Analysis*, Vol.20, 1985, 104-105
- Picon, M., Vichy, M., "D'Orient en Occident: l'origine du verre à l'époque romaine et durant le haut Moyen Age", in: Thirion-Merle, V. (eds.), *Échanges et commerce du verre dans le monde antique. Actes du colloque de l'Association Française pour l'Archéologie du Verre, Aix-en-Provence et Marseille, 7-9 juin 2001*, 2003, 17-31
- Pliny, *Natural History, Volume X: Books 36-37*, Translated by H. Rackham, Loeb Classical Library, 1938.
- Price, J., "Late Roman vessels in Britain, from AD 350 to 410 and beyond", in: Price, J. (eds.), *Glass in Britain and Ireland AD 350-1100*, British Museum Occasional Paper, No.127, 2000, 1-32
- Price, J., "Glass working and glassworkers in cities and towns", in: Mac Mahon, A., Price, J. (eds.), *Roman working lives and urban living*, 2005, 167-190
- Rebourg, A., "Les ateliers antiques, les fours d'Autun", in: Foy, D., Sennequier, G. (eds.), *A travers le verre, du Moyen Age à la Renaissance*, 1989, 49-52
- Rehren, T., "New aspects of ancient Egyptian glassmaking", *Journal of Glass Studies*, Vol.42, 2000, 13-24
- Ricciardi, P., "A non-invasive study of Roman Age mosaic glass tesserae by means of Raman spectroscopy", *Journal of Archaeological Science*, Vol.36, 2009, 2551-2559
- Ruggero, L., *L'opus sectile medievale in Sicilia e nel meridione normanno*, 2009, 1-156
- Rutten, F., Briggs, D., Henderson, J., Roe, M.J., "The application of time-of-flight secondary ion mass spectrometry (ToF-SIMS) to the characterization of opaque ancient glasses", *Archaeometry*, Vol.91, 2009, 66-86
- Sagúí, L., *Il vetro antico*, 2010
- Sanderson, D.C.W., Hunter, J.R., Warren, S.E., "Energy dispersive X-ray fluorescence analysis of 1st Millennium AD glass from Britain", *Journal of Archaeological Science*, Vol.11, 1984, 53-69
- Santagostino Barbone, A., Gliozzo, E., D' Acapito, F., Memmi Turbanti, I., Turchiamo, M., Volpe, G., "The Sectilia panels of Faragola (Ascoli-Satriono, southern Italy): A multi-analytical study of the red, orange and yellow glass slabs", *Archaeometry*, Vol.50, 2008, 451-473
- Sayre, E.V., Smith, R.W., "Compositional categories of ancient glass", *Science*, Vol.133, 1961, 1824-1826

- Schibille, N., Degryse, P., Corremans, M., Specht, C., "Chemical characterization of glass mosaic tesserae from sixth-century Sagalassos (south-west Turkey): chronology and production techniques", *Journal of Archaeological Science*, Vol.39, 2012, 1480-1492
- Schibille, N., Sterrett-Krause, A., Freestone, I., "Glass groups, glass supply and recycling in late Roman Cathage", *Archaeological Anthropological Science*, Vol.9, 2017, 1223-1241
- Shelby, J., *Introduction to Glass Science and Technology*, 2005
- Shepherd, J.D., Heyworth, M., "Le travail du verre dans Londres romain (Londinium): Un état de la question", *Ateliers de Verriers de l'antiquité a la période pré-industrielle*, Association Française pour l'archéologie du verre, Actes de 4emes Rencontres, Rouen, 24-25 Novembre 1989, 1991, 13-22
- Shortland, A.J., "The use and origin of antimonate colorants in Early Egyptian glass", *Archaeometry*, Vol.44 (4), 2002, 517-530
- Silvestri, A., Molin, G., Salviulo, G., "The colourless glass of Julia Felix", *Journal of Archaeological Science*, Vol.35, 2008, 331-41
- Slough, P.W., "The Art of Ancient Glass", *Bulletin of the Detroit Institute of Arts*, Vol.79, No.1(2), 2005, 34-45
- Starr, R.F.S., "Nuzi, report on the excavations at Yorgan Tapa near Kirkuk 1927-1931, 1939
- Stern, M., "Roman glassblowing in a cultural context", *American Journal of Archaeology*, Vol. 103, No.3, 1999, 441-484
- Stern, M., "Glass is Hot", *American Journal of Archaeology*, Vol.106, No.3, 2002, 463-471
- Stern, M., "Blowing glass from chunks instead of molten glass: Archaeological and literary evidence", *Journal of Glass Studies*, Vol.54, 2012, 33-45
- Strabo, *Geography*, Translated by A. Meineke, Perseus Digital Library, 1877
- Suetonius, *De vitae Caesarum*, Translated by J.C. Rolfe, Loeb Classical Library, 1914
- Tacitus, *Annales*, Translated by J. Jackson, Loeb Classical Library, 1925
- Tal, O., Jackson-Tal, R.E., Freestone, I., "New evidence of the production of raw glass at late Byzantine Apollonia-Arsurf, Israel", *Journal of Glass Studies*, Vol.46, 2004, 51-66
- Tesser, E., Verità, M., Lazzarini, L., Falcone, R., Saguí, L., Antonelli, F., "Glass in imitation of exotic marbles: An analytical investigation of 2nd century AD Roman sectilia from the Gorga collection", *Journal of Cultural Heritage*, Vol.42, 2020, 202-212

Tite, M.S., Shortland, A.J., Production technology of faience and related early vitreous materials, 2008

Triantafyllidis, P., "Classical and Hellenistic glass from Rhodes", in: Foy, D., Nenna, M.D. (eds.), *Échanges et commerce du verre dans le monde antique* (colloque de l'AFAV, Aix-en-Provence, Marseille 2001), *Monographies Instrumentum*, Vol.24, 2003, 131-138

Varro, M.T., *De Re Rustica*, Translated by W.D. Hooper, H.B. Ash, Loeb Classical Library, 1934

Verità, M., Arena, M.S., Carruba, A., Santopadre, P., "Roman glass: Art and technology in a 4th century A.D. opus sectile in Ostia (Rome)", *Journal of Cultural Heritage*, Vol.9, 2008, 16-20

Verità, M., Maggetti, M., Saguí, L., Santopadre, P., "Colors of Roman glass: An Investigation of the yellow sectilia in the Gorga Collection", *Journal of Glass Studies*, Vol.55, 2013, 39-52

Verità, M., Santopadre, P., "Unusual glass tesserae from a third-century mosaic in Rome", *Journal of Glass Studies*, Vol.57, 2015, 287-292

Wainwright, I., Taylor, J., Harley, R., "Lead antimonate yellow", *Artists' Pigments. A Handbook of their History and Characteristics*, Vol.1, 1986, 219-254

Wedepohl, K.H., "The change in composition of medieval glass types occurring in excavated fragments from Germany", *Proceedings of the 14th Congress of the International Association for the History of Glass*, 2000, 253-257